Rev. Neurosci., Vol. 22(4): 373–402, 2011 • Copyright © by Walter de Gruyter • Berlin • Boston. DOI 10.1515/RNS.2011.035

Hippocampal synaptic plasticity in Alzheimer's disease: what have we learned so far from transgenic models?

Cristina Marchetti[1] and Hélène Marie[1,2,*]

[1] Laboratory of Molecular Mechanisms of Synaptic Plasticity, European Brain Research Institute, I-00143 Rome, Italy
[2] Institut de Pharmacologie Moléculaire et Cellulaire (IPMC), UMR6097 CNRS/UNSA, F-06560 Valbonne, France

*Corresponding author
e-mail: marie@ipmc.cnrs.fr

Abstract

Transgenic (Tg) mouse models of Alzheimer's disease (AD) are used to investigate mechanisms underlying disease pathology and identify therapeutic strategies. Most Tg AD models, which at least partly recapitulate the AD phenotype, are based on insertion of one or more human mutations (identified in Familial AD) into the mouse genome, with the notable exception of the anti-NGF mouse, which is based on the cholinergic unbalance hypothesis. It has recently emerged that impaired hippocampal synaptic function is an early detectable pathological alteration, well before the advanced stage of amyloid plaque accumulation and general cell death. Nevertheless, electrophysiological studies performed on different Tg models or on the same model by different research groups have yielded contrasting results. We therefore summarized data from original research papers studying hippocampal synaptic function using electrophysiology, to review what we have learned so far. We analyzed results obtained using the following Tg models: (1) single/multiple APP mutations; (2) single presenilin (PS) mutations; (3) APPxPS1 mutations; (4) APPxPS1xtau mutations (3xTg); and (5) anti-NGF expressing (AD11) mice. We observed that the majority of papers focus on excitatory basic transmission and long-term potentiation, while few studies evaluate inhibitory transmission and long-term depression. We searched for common synaptic alterations in the various models that might underlie the memory deficits observed in these mice. We also considered experimental variables that could explain differences in the reported results and briefly discuss successful rescue strategies. These analyses should prove useful for future design of electrophysiology experiments to assess hippocampal function in AD mouse models.

Keywords: Alzheimer's disease; hippocampus; synaptic plasticity; transgenic mouse.

Introduction

Transgenic (Tg) mouse models that recapitulate a range of Alzheimer's disease (AD)-like phenotypes have been used for over 15 years to investigate mechanisms underlying disease pathology. Most Tg AD mouse models have been engineered by the insertion in the mouse genome of mutated human genes, first identified in early-onset familial cases of AD (FAD).

One of the factors associated with AD is the aberrant processing of the amyloid precursor protein (APP), which leads to increased levels of the Aβ peptide, one of its proteolytic derivatives. The most common isoforms of Aβ are Aβ40 and Aβ42, with Aβ42 being more fibrillogenic and thus aggregating into insoluble plaques within the brain, a phenomenon that is one of the hallmarks of the pathology. Another prominent pathological hallmark of AD is the presence of hyperphosphorylated tau, a microtubule associated protein, which, when aggregating, forms neurofibrillary tangles (NFTs), typical of taupathies. AD is also characterized by neuronal loss, with cholinergic neurons of the basal forebrain being especially sensitive and representing the first cell population to die during disease progression. Understanding how these different aspects of the pathology contribute to the debilitating AD-related memory loss is a matter of intense investigation. In recent years, however, evidence has accumulated demonstrating that synaptic loss, rather than Aβ plaques, NFTs or neuronal loss, is the best pathological correlate of cognitive impairment (Selkoe, 2002; D'Amelio et al., 2011). In particular, impaired synaptic function of the hippocampus appears to be particularly affected, leading to defective hippocampal-dependent memory processing, well before the advanced stage in which amyloid plaques accumulate and general cell loss takes place. Within the last two decades, several electrophysiological studies have therefore been performed on Tg AD models to identify the nature of this defect.

In this review, we have analyzed all the original research papers that we could identify, which report *in vitro* slice or *in vivo* analysis of hippocampal synaptic function using electrophysiology from the following groups of Tg mouse models: (1) APP-derived; (2) single presenilin (PS)-derived; (3) APPxPS1; (4) APPxPS1xTau (3xTg); (5) anti-NGF expressing (AD11) mice. We have chosen to focus on these AD mouse models as they have been the most promising in reproducing at least some of the hallmarks of the disease.

We have searched for common denominators of synaptic alterations across the different Tg models that could provide new insights into hippocampal dysfunctions underlying the memory deficits observed in these mice. We also report

rescue strategies evaluated so far and experimental variables that could explain differences in conflicting results.

Description of the AD mouse models

Several mouse models have been evaluated for hippocampal function by means of electrophysiology. For clarity, we divide them throughout the review in APP-derived, PS1-derived, APP/PS1, 3xTg and AD11 models (Table 1). In this section, we will briefly review the genotypes and the phenotypes of all the models used for the electrophysiological studies. A summary of the information and the references, as well as complementary information on these models, is reported in Table 1. This table does not represent an exhaustive list of AD mouse models available, but only models analyzed by electrophysiology. For a more comprehensive review on AD mouse models, one can refer to the following papers: Ashe and Zahs, 2010; Elder et al., 2010; Morrissette et al., 2009 or visit the Alzheimer forum at http://www.alzforum.org/res/com/tra/default.asp.

APP-derived models

These mice over-express the human form of APP, mutated in one or more sites (see Table 1 for mutation details and references). The single mutations inserted in the APP gene represent mutations characterized in FAD, which are named the Swedish (swe), the Indiana (ind), the London (Ld) or arc mutations. Another set of mice harbor the swe mutation together with either the ind or arc mutation. With aging, these models exhibit Aβ accumulation and plaques, hyperphosphorylated tau, and hippocampal-dependent memory deficits reminiscent of AD pathology, but do not display NFTs, cholinergic deficits or neuronal loss (Morrissette et al., 2009).

PS1-derived models

Most of these mice over-express the human presenilin gene (PS1) harboring an FAD mutation. This gene is implicated in the proteolysis of APP as part of the γ-secretase complex. The mutations are named by the amino acid change that they result in (see Table 1 for mutation details and references). Studies of electrophysiology have been performed on mutants M146L, M146V, A246E and L286V. A mouse model was also generated encoding the PS1ΔE9 FAD mutation, which results in a non-cleavable, but functional, variant of PS1. One knock-in mouse was generated where mouse PS1 was replaced by its mutant M146V. These presenilin FAD mutant mice consistently show an age-dependent elevation of Aβ42 with little effect on Aβ40, but they generally do not develop plaques, tau pathology, cholinergic deficits or neuronal loss and have few cognitive deficits (Games et al., 2006).

APP/PS1 models

To increase the brain Aβ accumulation and plaque load, several investigators crossed APP-derived and PS1-derived mouse models. Most double transgenic models studied by electrophysiology harbored the human APPswe transgene together with the PS1M146L, the PS1A246E, the PS1L166P or the PS1Δ9 transgene (see Table 1 for details and references). One knock-in mouse was generated where the mouse APP gene harbors the swe mutation along with missense mutations (to humanize mouse Aβ) and the PS1 gene harbors the L166P mutation. APP/PS1 double transgenic mice generally develop early and extensive Aβ plaque formation and exhibit tau hyperphosphorylation and cognitive deficits, but still lack cholinergic deficits, neuronal loss and NFTs (Morrissette et al., 2009).

3xTg model

The 3xTg model over-expressing human APPswe and tau MAPTP301L and harboring a knock-in of PS1M146V was engineered by Oddo et al. (2003). With aging, these mice display both Aβ plaques and tangle pathology, including NFTs, and exhibit hippocampal-dependent memory deficits. They also exhibit cholinergic alterations and cortex-specific neuronal loss (Oddo et al., 2003; Bittner et al., 2010; Perez et al., 2011).

AD11 model

This alternative model is not based on FAD mutations, but on the long-standing hypothesis that AD pathology might be due to loss of neurotrophic action of the nerve growth factor (NGF) (Capsoni and Cattaneo, 2006). These mice express an anti-NGF antibody which reduces the levels of free NGF from about 1.5 months of age (Capsoni et al., 2000). With aging, these mice display all lesions of AD pathology including Aβ accumulation and plaques, tau hyperphosphorylation and NFTs, cholinergic deficits and hippocampal-dependent memory deficits.

Before describing the functional hippocampal alterations observed in these mice models, we will briefly introduce the hippocampal system.

The hippocampal system

The hippocampus is a highly organized structure playing a major role in memory encoding and spatial navigation (Kesner and Hopkins, 2006). It is one of the first regions of the brain to suffer damage in Alzheimer's disease (Karow et al., 2010). It is characterized by the tri-synaptic pathway consisting of three glutamatergic synapses, which relay information from the entorhinal cortex (EC) to CA1 cells (Figure 1). The main input to the hippocampus is the perforant pathway emanating from the EC, which forms excitatory synapses with the granule cells of the dentate gyrus (DG). It is divided into two sets of fibers: the medial and the lateral perforant pathways (MPP and LPP, respectively). The first one is generated at the medial portion of the entorhinal cortex and makes connections onto the proximal dendritic area of the granule cells; the latter is generated at the lateral portions of the entorhinal

Table 1 Transgenic AD mouse models evaluated for hippocampal function by electrophysiology.

Mouse name	Mutated gene and name of mutation	Mutated amino acids (promoter)	Background	Original description of mouse	Synaptic plasticity – *in vivo*	Synaptic plasticity – *in vitro*
APP-derived models						
TG2576 (or APPsw or APPswe)	Human APP695 with Swedish mutation	K670N/M671L (PrP)	C57BL/6JxSJL	Hsiao, 1996	1) Mitchell, 2009; 2) Chapman, 1999; 3) Matsuyama, 2007	1) Chapman, 1999; 2) Fitzjohn, 2001; 3) Trinchese, 2004; 4) Jacobsen, 2006; 5) D'Amelio, 2011
APP23	Human APP751 with Swedish mutation	K670N:M671L (Thy1.2)	C57BL6 (for Roder, 2003)	Sturchler-Pierrat, 1997	1) Huang, 2006	1) Roder, 2003; 2) Middei, 2010
TAS10	Human APP695 with Swedish mutation	K670N:M671L (Thy1)	Not specified	Richardson, 2003		1) Brown, 2005
APP/Ld	Human APP695 with London mutation	V717I (Thy1) (also called V642I if numbering of APP695)	FVB/N	Moechars, 1999		1) Moechars, 1999; 2) Dewachter, 2002; 3) Postina, 2004; 4) Dewachter, 2009
APPind H6	Human APP695-770-771 with Indiana mutation (PDGF-hAPP transgene also called PDAPP minigene)	V717F (PDGF)	C57BL6×DBA2	Wyss-Coray, 1997		1) Hsia, 1999
PDAPP/109	Human APP695-770-771 with Indiana mutation (PDGF-hAPP transgene also called PDAPP minigene)	V717F (PDGF)	Swiss webster×C57BL6×DBA2	Games, 1995	1) Giacchino, 2000	1) Larson, 1999; 2) Hartman, 2005
hAPPJ9 and hAPPJ20 (APPswe, ind or PDAPPJ9)	Human APP695-770-771 with Swedish+Indiana mutations (from PDAPP minigene)	K670N:M671L, V717F (PDGF)	Early papers: C57BL6×DBA2 recent papers: C57BL6	Line J9: Hsia, 1999, Line J20: Mucke, 2000		1) Saganich, 2006; 2) Palop, 2007; 3) Sun, 2008; 4) Dziewczapolski, 2009; 5) Harris, 2010; 6) Cissé, 2011; 7) Roberson, 2011
TgCRND8	Human APP695 with Swedish+Indiana mutations	K670N:M671L, V717F (PrP)	C57BL6 (75%)×C3H (25%)	Chishti, 2001		1) Jolas, 2002
ArcAbeta	Human APP695 with Swedish+arc mutations	K670N:M671L, E693G (PrP)	C57BL6×DBA2	Knobloch, 2007b		1) Knobloch, 2007a
PS1-derived models						
PS1 M146L	Human PS1 with ML146L mutation	ML146L (PDGF)	SW×B6D2F1	Duff, 1996		1) Barrow, 2000; 2) Trinchese, 2004
PS1 M146V	Human PS1 with ML146V mutation	ML146V (PDGF)	SW×B6D2F1	Duff, 1996		1) Barrow, 2000
PS1 A246E	Human PS1 with A246E mutation	A246E (PrP)	B6C3F1	Borchelt, 1996		1) Parent, 1999
PS1A246E (PS1/Mut/2)	Human PS1 with A246E mutation	A246E (Thy1)	FVB/N	Schneider, 2001		1) Schneider, 2001; 2) Dewachter, 2008
PS1 Delta Exon 9 (PS1 dE9)	Human PS1 with deletion of Exon 9	Delta-E9 (PrP)	B6C3F1	Lee, 1997		1) Zaman, 2000
PS1L286V (mutPS1)	Human PS1 with L286V mutation	L286V (PrP)	C57BL6	Citron, 1997		1) Auffret, 2009
PS1M146V KI	PS1 M146V Knock in	M146V (endogenous promoter)	C57BL6×129	Guo, 1999		1) Oddo, 2003; 2) Wang, 2009; 3) Auffret, 2010

Table 1 (Continued)

Mouse name	Mutated gene and name of mutation	Mutated amino acids (promoter)	Background	Original description of mouse	Synaptic plasticity – *in vivo*	Synaptic plasticity – *in vitro*
APP/PS1 models						
APPswe/PS1M146L	Cross of Tg2576×PS1M146L mice	hAPP-K670N: M671L (PrP) and hPS1-M146L (PrP)	C57BL/6J×SJL×DBA×SW	Tg2576: Hsiao, 1996; PS1M146L: Duff, 1996		1) Trinchese, 2004; 2) Knobloch, 2007a; 3) Trinchese, 2008
APPswe/PS1M146V	Cross of Tg2576×PS1M146V mice	hAPP-K670N: M671L (PrP) and hPS1-M146V (PrP)	C57BL/6J×SJL×DBA×SW	Tg2576: Hsiao, 1996; PS1M146V: Duff, 1996		1) Gong, 2004
APPswe/PS1A246E	Cross of Mo/Hu APP695swe×PS1A246E	hAPP-K670N: M671L (PrP) and hPS1-A246E (PrP)	APPswe: [C3H/HeJ 3 C57BL/6J F3]×C57BL/6J n1 PS1-A246E: C3H/HeJ×C57BL/6J F	Mo/Hu APPswe: Borchelt, 1996; PS1A246E: Borchelt, 1996	1) Gureviciene, 2004	1) Gureviciene, 2004; 2) Fitzjohn, 2010
APPswe/PS1L166P (APPPS1-21)	APP695swe and PS1 L166P (co-injected to make new transgenic line)	hÄPP-K670N: M671L (Thy-1) and hPS1L-166P (Thy1)	C57BL6	Radde, 2006	1) Gengler, 2010	1) Calella, 2010
APPswe/PS1ΔE9	Mo/Hu APP695swe and PS1dE9 (co-injected to make new transgenic line)	hAPP-K670N: M671L (PrP) and hPS1 dE9 (PrP)	C57BL6	Jankowsky, 2003		1) Yoshiike, 2008; 2) Volianskis, 2010
APPNLh/PS1P246L (2×KI)	Endogenous APPswe and additional missense mutations to humanize mouse Abeta and endogenous mutation P264L in PS1 mouse gene	Endogenous APP-K670N:M671L:missense mutations and PS1L166P	129×CD1	Flood, 2002		1) Chang, 2006
3×TG model						
3×Tg	APP695swe, PS1 M146V KI and MAPT with P301L mutation	APP-K670N/M671L, MAPT-P301L (both Thy2.1) and PS1-M146V KI (endogenous promoter)	C57BL6/129	Oddo, 2003		1) Oddo, 2003; 2) Wang, 2009
Anti-NGF model						
AD11	Expresses recombinant version of monoclonal antibody αD11 against NGF by cross of homozygous VH (heavy chain)-αAD11 line with homozygous VK (light chain)-αAD11 line	VHαD11 (CMV) and VKαD11 (CMV)	C57BL6×SJL	Ruberti, 2000		1) Rosato-Siri, 2006; 2) Sola, 2006; 3) Lagostena, 2010; 4) Houeland, 2010

The Table summarizes information relative to transgenic AD mouse models, for which hippocampal electrophysiological studies were performed. We report the mouse names that are generally used and to which we refer in this review (column 1), the transgene (or endogenous mutation) and name of mutation (column 2), the mutated amino acid sequence and promoter used to drive the transgene (column 3) and the background on which the model mice were bred (column 4). For each model, we also report the reference to the first mouse description (column 5) and all the references to the studies that performed electrophysiology *in vivo* (column 6) or *in vitro* (column 7) discussed in this review (only lead author names are given). Models were grouped into APP-derived, PS1-derived, APP/PS1, 3xTg and AD11 models.

For Reference citation only lead names are given in all Tables.

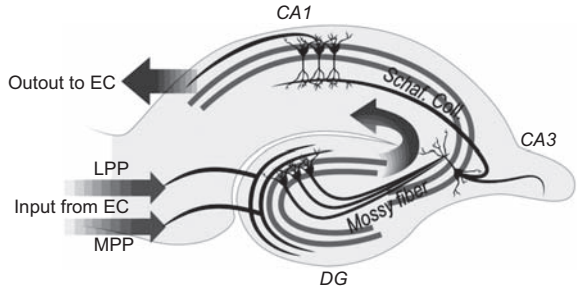

Figure 1 Diagram of the hippocampus displaying the glutamatergic tri-synaptic pathway (DG, CA3, CA1).
EC, enthorinal cortex; LPP, lateral perforant pathway; MPP, medial perforant pathway; Schaf. Coll., Schaffer collateral fibers.

cortex and synapses onto the distal dendrites of these same cells. The MPP and LPP synapses have different properties (e.g., inverse short-term plasticity phenotype), but investigators do not systematically differentiate between the two incoming pathways during their recordings, leading to difficulties in comparison of data. From DG granule cells, axons forming the mossy fiber pathway connect to the pyramidal cells in area CA3, which in turn project to the pyramidal cells in CA1 by means of the Schaffer collateral pathway. We will refer to this latter connection as the SC-CA1 synapse throughout the review. The excitability of the tri-synaptic pathway is tightly regulated by the activity of local interneurons which synapse onto excitatory neurons. These interneuron-excitatory neuron synapses release the inhibitory neurotransmitter γ-aminobutyric acid (GABA) and control the depolarizing potential of the excitatory neurons.

Virtually all studies have focused on the SC-CA1 and/or the DG synapses. Only two papers report analysis of synaptic activity in CA3 neurons (Barrow et al., 2000; Brown et al., 2005). We have divided the following sections by type of hippocampal function that was analyzed and provide a brief explanation of each function before summarizing the data reported in the different AD mouse models. We have also divided the reporting of data by synapse analyzed and by AD model type in sections where a large body of literature was available.

Basic glutamatergic synaptic transmission

The main type of excitatory transmission in the hippocampus is *via* release of glutamate from the pre-synaptic terminals leading to the binding and opening of α-amino-3-hydroxy-5-methylisoazol-4-propionate and *N*-methyl-D-aspartate ionotropic receptors (AMPAR and NMDAR) at the post-synaptic terminal. At resting membrane potential, NMDAR channel opening is blocked by Mg^{2+} leaving the AMPARs as the main contributors to the transmission. Synaptic responses can be recorded by field or single cell recording techniques. In the field configuration, the synaptic response from a population of neurons is recorded as a variation in the potential (field excitatory post-synaptic potential or fEPSP). In single cell recording, synaptic responses are usually recorded with the voltage-clamp whole cell technique. In this configuration, current excitatory synaptic currents (EPSC) are recorded.

For a rapid assessment of the status of synaptic transmission, most investigators rely on fEPSP slope analysis in response to increasing stimulation of the afferent fibers. These measurements provide an input-output (I/O) relationship (or I/O curve). To minimize slice-to-slice recording variability (due to factors such as health and number of connections within the slice, electrode position and tip size, etc.), fEPSPs are usually reported relative to the pre-synaptic fiber volley (FV). The FV precedes the fEPSP in the recorded trace as it is the potential generated by the synchronous action potentials firing in the pre-synaptic fibers. An increase in the I/O curve suggests an increase in glutamatergic (mostly AMPAR-mediated) synaptic transmission, while a decrease in this parameter suggests impaired transmission. FV and fEPSP amplitudes are also sometimes reported, but since they are highly variable between slices and preparations, their alterations are more difficult to interpret. One can isolate the AMPAR or NMDAR currents by using pharmacological blockers of either channel to assess receptor-specific I/O relationships and roughly evaluate the relationship between the two currents or field potentials. Again, to take into account variability in the recording conditions between slices, the ratio between AMPAR-mediated and NMDAR-mediated currents (more common) or fields can be reported.

Another protocol useful to assess changes in glutamatergic transmission is the recording of spontaneous or miniature EPSCs (sEPSCs and mEPSCs, respectively), which can only be performed during whole cell recordings. sEPSCs are usually due to release of one vesicle containing glutamate (quantum) from the pre-synaptic terminal. This release can be either triggered by action potential-firing in the pre-synaptic neuron, or action potential-independent. If a sodium channel blocker like tetrodotoxin (TTX) is added to the recording medium, only action potential-independent events, called miniature EPSC (mEPSC), will take place. At resting membrane potential, due to the NMDAR Mg^{2+} block, spontaneous release of glutamate will generate only AMPAR EPSC. Due to quantal release, a change in the amplitude of mEPSCs or sEPSC is generally interpreted as a variation in the number of AMPARs per synapse. On the contrary, an alteration in event frequency can be interpreted as due to changes in the number of spontaneous release events from the pre-synaptic terminal or to a change in the number of synapses containing AMPARs. NMDAR spontaneous mEPSC analysis is only very rarely reported because the events' slow rise time and low amplitude make accurate and reliable detection difficult. To our knowledge, it has never been reported for AD mouse models.

Basic synaptic transmission in AD models: SC-CA1 synapse

Table 2 summarizes the analysis of basic synaptic transmission at the SC-CA1 synapse from AD models, obtained using field or whole cell electrophysiology. After 15 years of analysis of

Table 2 Evaluation of basic glutamatergic synaptic transmission at the hippocampal SC-CA1 synapse in AD Tg models.

							Color legend:	Normal	Decrease	Increase	Rescued	Not rescued
In vitro							Months of age					
Paper	Mouse	Protocol	Kyn	GB	S/I	Ca	n.s.	1	2	3	4	5	6	7	8	9	10	11	12	13	14	15	16	17	18	19	20	≥24
Chapman, 1999	Tg2576	Field I/O	Yes	No	S	2.5																						
Fitzjohn, 2001	Tg2576	Field I/O	No	No	S	2.4																						
		Field I/O	Yes	No	S	2.4																						
Trinchese, 2004	Tg2576	Field I/O	Yes/No	No	n.s.	2					*	*	*	*														
D'Amelio, 2011	Tg2576	Field I/O	No	P	S	2.5																						
D'Amelio, 2011	Tg2576	**AMPA/NMDA**	No	P	S	2.5																						
	Tg2576	***AMPA/NMDA+ casp. inh.***	No	P	S	2.5																						
	Tg2576	**miniAMPA freq**	No	P	S	4																						
	Tg2576	**miniAMPA amp**	No	P	S	4																						
Roder, 2003	APP23	Field I/O	No	No	I	2.5																						
Middei, 2010	APP23	Field I/O	No	No	S	2.4													*									
Brown, 2005	TAS10	Field I/O	No	No	I	2																						
Postina, 2004	APPLd2	Field I/O	No	No	S	n.s.																						
Larson, 1999	PDAPP/109	Field I/O	No	No	I	3.4																						
Hsia, 1999	APPind H6	Field I/O	No	P	S	2.5																						
	APPind H6	Field I/O	Yes	P	S	2.5																						
		AMPA/NMDA	No	P	S	2.5																						
		miniAMPA amp	No	P	S	2.5																						
	hAPPJ9	Field I/O	No	P	S	2.5																						
Dziewczapolski, 2009	hAPPJ9 (PDAPP J9)	Field I/O	Yes	No	S	2																						
Saganich, 2006	hAPPJ20	Field I/O	Yes	No	S	2																						
	D664A	Field I/O	Yes	No	S	2																						
		AMPA/NMDA	Yes	P	S	2																						
Palop, 2007	hAPPJ20	Field I/O	No	P+B	S	2																						
Sun, 2008	hAPPJ20	Field I/O	No	No	S	2																						
	hAPPJ20/CST3-/-	Field I/O	No	No	S	2																						
Harris, 2010	hAPPJ20	Field I/O	No	No	S	2																						
	D664A	Field I/O	No	No	S	2																						
Cissé, 2011	hAPPJ20	Field I/O	No	No	S	2																						
	hAPPJ20 with EphB2 lenti	Field I/O	No	No	S	2																						
Roberson, 2011	hAPPJ20	Field I/O	No	No	S	2																						
	hAPPJ20/Tau-/-	Field I/O	No	No	S	2																						
Dewachter, 2009	APPLd2	Field AMPA I/O	No	No	I	2.4																						
		Field NMDA I/O	No	No	I	2.4																						
Jolas, 2002	TgCRND8	Field I/O	No	No	S	2.5																						
	TgCRND8	Field I/O	No	B	S	2.5																						

Table 2 (Continued)

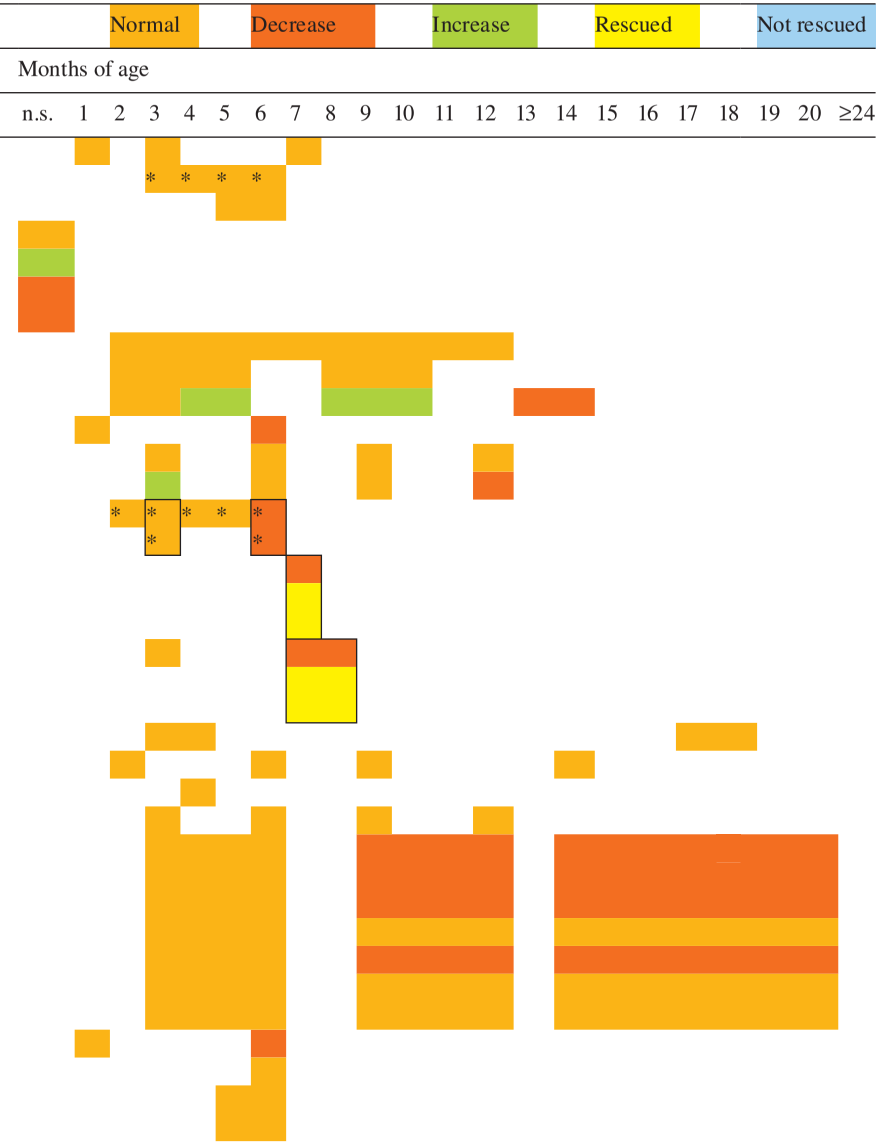

In vitro							
Paper	Mouse	Protocol	Kyn	GB	S/I	Ca
Knobloch, 2007a	ArcBeta	Field I/O	No	No	I	2.5
Trinchese, 2004	PS1M146L	Field I/O	Yes/No	No	n.s.	2
Parent, 1999	PS1A246E	Field I/O	No	No	I	2
Dewachter, 2008	PS1A246E	Field AMPA I/O	No	No	n.s.	2.4
	PS1A246E	Field NMDA I/O	No	No	n.s.	2.4
	PS1A246E	Field AMPA/ NMDA	No	No	n.s.	2.4
Zaman, 2000	PS1ΔE9	Field I/O	No	No	S	2.5
Auffret, 2009	PS1L286V	Field AMPA I/O	No	P	S	2
		Field NMDA I/O	No	P	S	2
Oddo, 2003	PS1M146V KI	Field I/O	No	No	I	2
Auffret, 2010	PS1M146V KI	Field AMPA I/O	Yes	P	S	2.5
		Field NMDA I/O	Yes	P	S	2.5
Trinchese, 2004	APPswe/PS1M146L	Field I/O	No	No	n.s.	2
		Field I/O	Yes	No	n.s.	2
Trinchese, 2008	APPswe/PS1M146L	Field I/O	No	P	n.s.	2
	APPswe/PS1M146L	Field I/O+calpain inhibitor	No	P	n.s.	2
Gong, 2004	APPswe/PS1M146V	Field I/O	No	No	n.s.	2
		Field I/O+ rolipram	*No*	No	n.s.	2
Gureviciene, 2004	APPswe/PS1A246E	Field I/O	No	No	I	3.4
Fitzjohn et al., 2010	APPswe/PS1A246E	Field I/O	No	No	n.s.	2.4
Calella, 2010	APPswe/PS1L166P	Field I/O	No	No	I	2.5
Volianskis, 2010	APPswe/PS1ΔE9	Field I/O	No	No	S	2
Chang, 2006	APPNLh/PS1P246L	Field I/O	Yes	P	S	2.4
		Evoked AMPA EPSC	Yes	P	S	2.4
		miniAMPA freq	No	P	S	2.4
		miniAMPA amp	No	P	S	2.4
		Evoked NMDA EPSC	Yes	P	S	2.4
Oddo, 2003	3xTg	Field I/O	No	No	I	2
Rosato-Siri, 2006	AD11	Field I/O	No	No	S	2
Sola, 2006	AD11	**miniAMPA freq**	No	No	S	2
	AD11	**miniAMPA amp**	No	No	S	2

Table 2 (Continued)

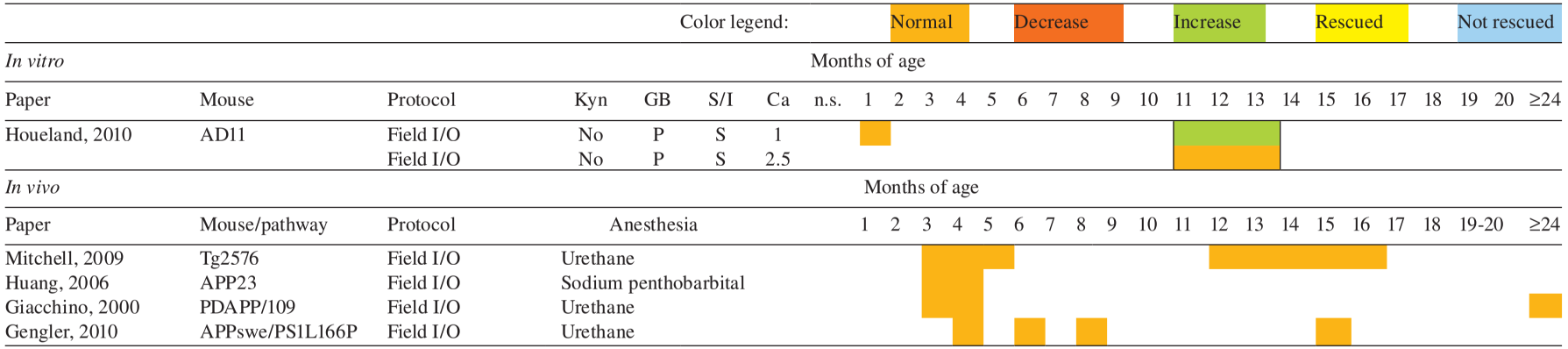

Results obtained in Tg mice are reported as comparisons against their respective wild-type phenotypes (normal, decrease or increase) through color coding (see top of Table), in an age-dependent manner. Studies were divided into *in vitro* and *in vivo*. Attempts of rescue (in italics in mouse or protocol column) are also reported in color codes (see top of Table; casp. inh, caspase inhibitor). We report the protocol used to assess basic synaptic transmission (see text for details). Field AMPA recordings were performed in the presence of the NMDAR blocker APV, while field NMDA experiments were made in the presence of AMPAR blockers. For EPSC analysis: freq, frequency; amp, amplitude. Experiments done in whole cell configuration are highlighted by bold writing in the 'protocols' column. For *in vitro* studies, we also detail the recording conditions: 'Kyn' indicates the presence of kynurenate during the dissection (y, yes; y/n indicates results were the same whether experiments were performed in kynurenate or not); 'GB' indicates the presence of the $GABA_A$ergic blockers, picrotoxin (P) or bicuculline (B), during recordings; 'S/I' refers to recordings in a submerged or interface chamber. The 'Ca' column reports ACSF Ca^{2+} concentration used during experiments. 'n.s.', not specified. The asterisk indicates that electrophysiology experiments were performed after behavior protocols. For *in vivo* experiments, the anesthesia under which recordings were performed is specified. Colored boxes surrounded by black contours highlight direct comparison of a parameter by the same experimenter (e.g., for rescue experiments or recording condition).

this synaptic function, the emerging picture is still not clear. For each study presented in Table 2, we report some of the experimental conditions that might influence results. These are: (1) the presence of kynurenate during the dissection; (2) the presence of $GABA_A$ receptor blockers during recordings; (3) recording in a submerged or interface chamber; (4) extracellular Ca^{2+} concentration.

APP-derived models

Even at similar ages and sometimes in apparently identical slicing and recording conditions, the twenty studies on the different APP-based models analyzing I/O relationship at the SC-CA1 synapse provide highly conflicting results. Notably, contrasting results were even found in the same mouse model (see Table 2, e.g., Chapman et al., 1999 vs. Fitzjohn et al., 2001 for the Tg2576 model or Roder et al., 2003 vs. Middei et al., 2010 for the APP23 model). As detailed in Table 2, most studies (14/20) report analysis between 3 and 10 months of age. Even in this age range, about half of the papers (6/14) report normal I/O relationship while the other half (8/14) observed reduced basic transmission. In the few studies (7/20) that analyzed this transmission in older animals (12 months onwards), a conflict in the data reported is still apparent. Some of these studies performed electrophysiological recordings after behavioral tests (Trinchese et al., 2004; Middei et al., 2010), a sequence that in principle could unmask subtle deficits present only in the AD mouse model. Impairment in I/O curves was not detected by Middei et al. in APP23 mice after training the animals in the Morris water maze (when compared to pseudo-trained mice) nor in Trinchese et al. after training in the radial arm water maze test, suggesting that this parameter of synaptic function is not affected by previous engagement of the hippocampus in memory formation.

Data from whole cell electrophysiology performed on APP-derived models can also reveal subtle alterations that are not apparent with field I/O recordings, as in our recent study on 3-month-old Tg2576 mice where we observed normal field I/O relationship, but lower AMPA/NMDA ratios and lower AMPA mEPSC frequency (D'Amelio et al., 2011). The lowering of this ratio was first described in another APP-derived model by Hsia et al. (1999), but not confirmed by Saganich et al. (2006). It is worth noting that, contrary to our study, Saganich et al. (2006) report a reduction in field I/O and no change in the AMPA/NMDA ratio. In the Saganich et al. study, however, picrotoxin was present only in whole cell and not in field recordings, thereby making the comparison difficult (see Table 2 for details). We and others also report normal AMPA mEPSC amplitude in this type of model (Hsia et al., 1999; D'Amelio et al., 2011).

PS1-derived models

Only four reports analyzed the I/O relationship in PS1-derived models with analysis spanning over 1–12-month-old mice (see Table 2 for references and details). Within this age range, most studies (3/4) reported normal synaptic transmission at the SC-CA1 synapse, while only Oddo et al. (2003) report reduced transmission correlating with aging. Mice submitted to a memory task before electrophysiological analysis did not display alterations (Trinchese et al., 2004). No data are available on I/O relationships in PS1 mutants older than 1 year. Three studies isolated the AMPAR and NMDAR fEPSP. They reported normal AMPAR I/O relationships at all ages analyzed. However, they observed age-dependent alterations of NMDAR transmission, suggesting an early increase followed by a reduction in NMDAR transmission, although the age of appearance of these modifications was variable depending on the model evaluated (Dewachter et al., 2008; Auffret et al., 2009, 2010).

APP/PS1 models

Eight studies evaluated I/O relationships of the SC-CA1 synapse in APP/PS1 double transgenic mice (see Table 2 for references and details). Contrary to the early reduction observed in APP-derived models, all studies report normal I/O relationships up to at least 4 months of age and prior behavioral training of the mice did not influence this parameter at this age (Trinchese et al., 2004). After this age, about half of the reports (4/7) observed reduced transmission, but others (3/7) observed normal transmission. Chang et al. (2006) isolated the AMPAR and NMDAR components of the EPSC by whole cell electrophysiology and observed normal NMDAR, but reduced AMPAR transmission. They also report normal AMPA mEPSC frequency, but lower amplitude. These whole cell data contrast again with data reported in APP-derived models.

3xTg model

For the 3xTg model, Oddo et al. (2003) report reduced transmission by I/O field at 6 months but not 1 month of age. No independent study has confirmed or challenged this finding to date.

AD11 model

Another recording strategy that might reveal subtle changes in synaptic dysfunction is the lowering of $[Ca^{2+}]$ in the extracellular recording solution, a condition that decreases neurotransmitter release probability. We and others observed normal transmission at the SC-CA1 synapse in AD11 mice at 6 and 11–13 months of age in standard ($[Ca^{2+}]$=2.5 mM) external solution (Sola et al., 2006; Houeland et al., 2010). We, however, detected an enhancement of transmission at lower (1 mM) calcium concentration in 11–13-month-old mice, an alteration that was not present in 1-month-old mice (Houeland et al., 2010). This intriguing finding is supported by another recent study analyzing the effect of increasing endogenous Aβ (by treatment with thiorphan, a neprilysin inhibitor) on acute hippocampal slices (Abramov et al., 2009). This treatment leads to an increase in SC-CA1 synaptic transmission in low, but not high, calcium conditions. Together, these data suggest that this synapse might harbor an AD-related defect in the mechanism of pre-synaptic glutamate release, which is

sensitive to external calcium levels and only revealed under conditions of low release probability.

Contrary to *in vitro* studies, *in vivo* studies performed on the various models (Tg2576, APP23, PDAPP/109 and APPswe/PS1L166P) all report normal I/O relationship at the SC-CA1 synapse, arguing against any defect in synaptic transmission at this synapse *in vivo* (Giacchino et al., 2000; Huang et al., 2006; Mitchell et al., 2009; Gengler et al., 2010).

Considering the above analysis of the literature, at present it is not possible to argue for or against a significant effect of Aβ accumulation and resulting AD-like pathology on basic synaptic transmission at the SC-CA1 synapse. The only conclusion that we can draw from summarizing the conflicting data on APP and APP/PS1-based models is that, when a defect is detected at all, it is always a reduction in transmission, suggesting that Aβ accumulation under some experimental conditions might negatively affect this parameter. On the other hand, data suggest that FAD-related alterations in PS1 function do not overtly affect basic synaptic transmission of the AMPARs at the SC-CA1 synapse, but that NMDAR transmission might be more influenced with possibly a biphasic relationship leading first to enhancement of transmission and then a reduction. Finally, the data on AD11 mice suggest a potentially overlooked Aβ-linked calcium-dependent alteration of transmission that might uniquely occur in the aging brain in the context of decreasing cerebrospinal fluid (CSF) calcium levels (Jones and Keep, 1988). Re-analysis of other AD mouse models in 1 mM calcium conditions should help determine if this phenotype is unique to the AD11 model or if it is a more global Aβ-induced alteration as suggested by Abramov et al. (2009).

Basic synaptic transmission in AD models: DG synapse

The I/O relationship of glutamatergic transmission in the DG has been evaluated in only four AD models so far (see Table 3). While this makes it easier to summarize the data, fewer independent studies are present to confirm the findings. When a distinction was made as to what pathway was analyzed, the MPP was always evaluated. No data are available on the LPP. The only conflicting data regard the analysis of the Tg2576 model, where Chapman et al. (1999) and Fitzjohn et al. (2001) both report normal transmission up to 18 months of age, while Jacobsen et al. (2006) observe a decrease in transmission in this same model at 4–5 months of age. Brown et al. (2005) observed only a slight reduction in transmission at 12–14 months of age in TAS10 mice, also expressing hAPPswe. Analysis of hAPP/J20 mice consistently results in normal transmission, but this mouse model was only analyzed up to 6 months of age (Palop et al., 2007; Sun et al., 2008; Harris et al., 2010). Two other studies by Mucke's group in 4–6-month-old hAPPJ20 mice isolated the AMPAR and NMDAR potentials to individually evaluate their I/O relationship and both report normal AMPAR transmission but reduced NMDAR transmission (Cissé et al., 2011; Roberson et al., 2011). It is worth noting that the reduction in NMDAR transmission was not detectable in the standard measurement of the I/O relationship (no blockers) by the same investigators (Palop et al., 2007; Harris et al., 2010), most likely because AMPAR transmission dominates the EPSP during this standard analysis. Finally, we observed normal synaptic transmission at the MPP-DG synapse in 11–13-month-old AD11 mice, but as for the SC-CA1 synapse, we observed enhanced transmission in conditions of low release probability (Houeland et al., 2010). No analysis of DG transmission has ever been performed in PS1-derived and APP/PS1 models or 3xTg models.

The four papers reporting analysis of synaptic transmission in the DG *in vivo* in Tg2576, APP23, PDAPP/109 and APPswe/PS1A246E show normal I/O relationships (see Table 3), suggesting a lack of significant effects of AD-like pathology on this hippocampal parameter *in vivo*.

Together the available data on the DG synapses suggest that the development of AD-like pathology does not affect AMPAR transmission, but might compromise NMDAR transmission in the DG. Also, as for the SC-CA1 synapse, transmission might be altered in low calcium conditions. Further analysis of transmission at the DG synapses in other Tg models is required to confirm or challenge these findings.

Short-term pre-synaptic plasticity of AMPAR transmission

Hippocampal synapses display short-term plasticity, a process that modulates release of neurotransmitter by either enhancing it (facilitation), or by decreasing it (depression) (Zucker and Regehr, 2002). This short-term pre-synaptic plasticity occurs within a time-scale of milliseconds to a maximum of seconds and is highly dependent on calcium (Zucker and Regehr, 2002). The most commonly used assay to explore this plasticity is the paired-pulse ratio (PPR). A PPR protocol consists of delivering pairs of stimuli at one or more inter-stimulus intervals (ISI; 10 ms up to 500 ms in the studies reported here) and obtaining the ratio of the slope (and/or peak for whole cell recordings) of the second EPSP to the first EPSP (P2/P1). The SC-CA1 synapse of adult rodents typically displays paired-pulse facilitation (PPF) whereby the second response can be up to 150–200% larger than the first response. When recorded *in vitro*, DG granule cells typically display PPF (up to 150% increase) when the LPP is stimulated and paired-pulse depression (PPD; with up to 20% decrease) when the MPP is stimulated (McNaughton, 1980; Colino and Malenka, 1993). This short-term plasticity can also be evaluated when submitting the synapse to trains of stimulation at various frequencies. In this assay, one can assess more subtle alterations in synapse fatigue. As for the PPR assay, trains of stimulation lead to sustained facilitation at the SC-CA1 synapse and at the LPP-DG granule cell synapse, while they lead to sustained depression when stimulating the MPP to DG granule cell synapse (Houeland et al., 2010).

Short-term plasticity: SC-CA1 synapse

Out of the 28 studies which evaluate PPF at the SC-CA1 synapse *in vitro*, 25 report normal PPF, while only three report

Table 3 Evaluation of basic glutamatergic synaptic transmission at the hippocampal DG synapse in AD Tg models.

Color legend: Normal | Decrease | Increase | Rescued | Not rescued

In vitro

Paper	Mouse	Protocol	Pathway	Kyn	GB	S/I	Ca	Months of age: 1 2 3 4 5 6 7 8 9 10 11 12 13 14 15 16 17 18 ≥24
Chapman, 1999	Tg2576	Field I/O	n.s.	Yes	No	S	2.5	
Fitzjohn, 2001	Tg2576	Field I/O	MPP	Yes	P	S	2.4	
Jacobsen, 2006	Tg2576	Field I/O	n.s.	No	No	n.s.	n.s	
Brown, 2005	TAS10	Field I/O	MPP	No	No	I	2	
Palop, 2007	hAPPJ20	Field I/O	MPP	No	P+B	S	2	
Sun, 2008	hAPPJ20	Field I/O	MPP	No	Gab	S	2	
	hAPPJ20/CST3-/-	Field I/O	MPP	No	Gab	S	2	
Harris, 2010	hAPPJ20	Field I/O	MPP	No	P	S	2	
	D664A	Field I/O	MPP	No	P	S	2	
Cissé, 2011	hAPPJ20	Field AMPA I/O	MPP	No	P	S	2	
	hAPPJ20 with EphB2 lenti	Field AMPA I/O	MPP	No	P	S	2	
	hAPPJ20	Field NMDA I/O	MPP	No	P	S	2	
	hAPPJ20 with EphB2 lenti	Field NMDA I/O	MPP	No	P	S	2	
	hAPPJ20	**AMPA/NMDA***	MPP	No	P	S	2	
	hAPPJ20 with EphB2 lenti	AMPA/NMDA**	MPP	No	P	S	2	
	hAPPJ20	**miniAMPA amp**	MPP	No	P	S	2	
Roberson, 2011	hAPPJ20	Field AMPA I/O	MPP	No	P	S	2	
		Field NMDA I/O	MPP	No	P	S	2	
	hAPPJ20	**AMPA/NMDA**	MPP	No	**?**	S	2	
	hAPPJ20/Tau-/-	***AMPA/NMDA***	*MPP*	No	**?**	S	2	
	hAPPJ20	**AMPA current**	MPP	No	**?**	S	2	
	hAPPJ20	**NMDA current**	MPP	No	**?**	S	2	
	hAPPJ20/Tau-/-	***NMDA current***	*MPP*	No	**?**	S	2	
	hAPPJ20	**miniAMPA freq**	MPP	No	**?**	S	2	
	hAPPJ20/Tau-/-	**miniAMPA freq**	MPP	No	**?**	S	2	
	hAPPJ20	**miniAMPA amp**	MPP	No	**?**	S	2	
	hAPPJ20	**sAMPA freq**	MPP	No	**?**	S	2	
	hAPPJ20	**sAMPA amp**	MPP	No	**?**	S	2	
	hAPPJ20	**eEPSC amp**	MPP	No	**?**	S	2	
	hAPPJ20/Tau-/-	***eEPSC amp***	MPP	No	**?**	S	2	
Houeland, 2010	AD11	Field I/O	MPP	No	P	S	1	
		Field I/O	MPP	No	P	S	2.5	

Table 3 (Continued)

				Color legend:	Normal	Decrease	Increase	Rescued	Not rescued

In vivo					Months of age																		
Paper	Mouse/pathway	Protocol	Pathway	Anesthesia	1	2	3	4	5	6	7	8	9	10	11	12	13	14	15	16	17	18	≥24
Matsuyama, 2007	Tg2576	Field I/O	n.s.	Urethane																			
Huang, 2006	APP23	Field I/O	n.s.	Sodium penthobarbital																			
Giacchino, 2000	PDAPP/109	Field I/O	n.s.	Urethane																			
Gureviciene, 2004	APPswe/PS1A246E	Field I/O	n.s.	Awake																			

Results obtained in Tg mice are reported as comparisons against their respective wild-type phenotypes (normal, decrease or increase) through color coding (see top of table), in an age-dependent manner. Attempts of rescue (in italics in mouse or protocol column) are also reported in color codes (see top of table). Studies are divided into *in vitro* and *in vivo*. 'Pathway' indicates whether experiments were performed stimulating the medial or lateral perforant pathway (MPP or LPP). We report the protocol used to assess basic synaptic transmission (see text for details). Field AMPA recordings were performed in the presence of the NMDAR blocker APV, while field NMDA experiments were performed in the presence of AMPAR blockers. Experiments done in whole cell configuration are highlighted by bold writing in the 'protocols' column. For *in vitro* studies, we report recording conditions: 'Kyn' indicates the presence of kynurenate during the dissection (y: yes); 'GB' indicates the presence of the $GABA_A$ergic blockers, picrotoxin (P), bicuculline (B) or gabazine (Gab), during recordings; 'S/I' refers to recordings in a submerged or interface chamber. The 'Ca' column reports ACSF Ca^{2+} concentration used during experiments. 'n.s.', not specified. For *in vivo* experiments, the anesthesia under which recordings were performed is specified. For Cissé (2010): *experiments were done both in whole cell and field, obtaining the same results; **rescue experiments with the same protocol were done only in field. Colored boxes surrounded by black contours highlight direct comparison of a parameter by same experimenter (e.g., for rescue experiments or recording condition).

altered PPF (see Table 4A for details and references). We can therefore conclude that short-term plasticity of neurotransmitter release, as analyzed by the PPR, is unlikely to be significantly compromised at this synapse. Only a couple of studies have, however, evaluated this plasticity during trains of stimuli. Larson et al. (1999) report greater facilitation during trains of stimuli at 4–5 months and reduced facilitation at 24–29 months in PDAPP/109 mice. We also recently reported reduced facilitation during 40 Hz trains in 11–13-month-old AD11 mice, a phenotype not present at 1 month (Houeland et al., 2010). These data should be confirmed by independent studies and in other mouse models, but they demonstrate that eventuality of alterations in short-term plasticity of neurotransmitter release at the SC-CA1 synapse should not be completely dismissed as detection of these alterations might require more in depth analysis of this process than PPR measurements.

The three papers reporting *in vivo* evaluation of PPR at the SC-CA1 synapse report overall normal PPF except for minor alterations at a few inter-stimulus intervals (see Table 4A for references). We can therefore conclude that, as suggested by *in vitro* studies, if there is an alteration in neurotransmitter release at the SC-CA1 synapse, it is likely to be mild.

Short-term plasticity: DG synapses

Evaluation of PPR at DG synapses has only been reported by three groups on two types of mice (see Table 4B for details and references). Mucke's group identified a loss of facilitation in the MPP pathway as reported in four studies on 3–6-month-old hAPPJ20 mice (Palop et al., 2007; Harris et al., 2010; Cissé et al., 2011; Roberson et al., 2011). These data are, however, surprising as the MPP-DG synapse normally displays PPD (McNaughton, 1980; Colino and Malenka, 1993). Sun et al. (2008) observed a loss of facilitation in 3–4-month-old hAPPJ20 mice, but reported recording the LPP-DG synapse. Finally, we recently reported an age-dependent enhancement of depression at the MPP-DG synapse in AD11 mice starting around 3–4 months of age (Houeland et al., 2010). We further analyzed short-term plasticity during a 40 Hz train of stimuli and observed normal depression at the MPP-DG synapse in 1-month-old, but enhanced depression in 11–13-month-old AD11 mice (Houeland et al., 2010). Confirmation of a PPR alteration at DG synapses in other mouse models is necessary, but these first reports suggest that short-term plasticity of neurotransmitter release is likely to be more affected in the DG than in CA1. These data also warrant in-depth analysis of this plasticity to be performed.

Three studies report *in vivo* analysis of PPR in the DG. They provide mixed results, but comparison of these data is difficult as the exact pathway stimulated is not identified (Table 4B). These studies therefore do not help to confirm or disprove a defect of this type of plasticity in the DG.

Long-term potentiation of AMPAR transmission

The most studied form of long-term potentiation (LTP) observed in the hippocampus consists of an increase in the

Table 4 Short-term plasticity of glutamatergic synaptic transmission at the SC-CA1 (4A) and DG (4B) synapses of the hippocampus in AD mouse models.

Table 4A Short-term plasticity: SC-CA1.

Color legend: Normal | Decrease | Increase | Rescued | Not rescued

In vitro

Paper	Mouse	Observed		Kyn	GB	S/I	Ca	Months of age: n.s. 1 2 3 4 5 6 7 8 9 10 11 12 13 14 15 16 17 18 ≥24
Chapman, 1999	Tg2576	PPF		Yes	No	S	2.5	
Fitzjohn, 2001	Tg2576	PPF		No	No	S	2.4	
	Tg2576	PPF		Yes	No	S	2.4	
D'Amelio, 2011	Tg2576	**PPF**		No	P	S	2.5	
Middei, 2010	APP23	PPF		No	No	S	2.4	*
Brown, 2005	TAS10	PPF		No	No	I	2	
Larson, 1999	PDAPP/109	PPF		No	No	I	3.4	
	PDAPP/109	1, 5, 10 Hz	(fac.)	No	No	I	3.4	
Hsia, 1999	APPind H6	PPF		No	P	S	2.5	
Palop, 2007	hAPPJ20	PPF		No	P+B	S	2	
Saganich, 2006	hAPPJ20	PPF		Yes	No	S	2	
	D664A	PPF		Yes	No	S	2	
Harris, 2010	hAPPJ20	PPF		No	No	S	2	
	D664A	PPF		No	No	S	2	
Moechars, 1999	APPLd2	PPF		No	No	I	2.4	
Postina, 2004	APPLd2	PPF		No	No	S	n.s.	
Jolas, 2002	TgCRND8	PPF		No	No	S	2.5	
Parent, 1999	PS1A246E	PPF		No	No	I	2	
Schneider, 2001	PS1A246E	PPF		No	No	n.s.	2.4	
Dewachter, 2008	PS1A246E	PPF		No	No	n.s.	2.4	
Zaman, 2000	PS1ΔE9	PPF		No	No	S	2.5	
Auffret, 2009	PS1L286V	PPF		No	P	S	2	
Oddo, 2003	PS1M146V KI	PPF		No	No	I	2	
Wang, 2009	PS1M146V KI	PPF		No	No	S	2	
Auffret, 2010	PS1M146V KI	PPF		Yes	P	S	2.5	
Trinchese, 2004	APPswe/ PS1M146L	PPF		No	No	n.s	2	
Gureviciene, 2004	APPswe/ PS1A246E	PPF		No	No	I	3.4	
Fitzjohn, 2010	APPswe/ PS1A246E	PPF		No	No	S	2.4	
Chang, 2006	APPNLh/ PS1P246L	PPF		Yes	P	S	2.4	
Oddo, 2003	3xTg	PPF		No	No	I	2	
Rosato-Siri, 2006	AD11	PPF		No	No	S	2	
Houeland, 2010	AD11	PPF		No	P	S	2.5	
	AD11	40 Hz	(fac.)	No	P	S	2.5	

Table 4 (Continued)

				Color legend:	Normal			Decrease				Increase				Rescued			Not rescued			
In vivo					Months of age																
Paper	Mouse/ pathway	Observed	Anesthesia	n.s.	1	2	3	4	5	6	7	8	9	10	11	12	13	14	15	16	17	18	≥24
Giacchino, 2000	PDAPP/109	PPF	Urethane																			#
Huang, 2006	APP23	PPF	Sodium penthobarbital																			
Gengler, 2010	APPswe/ PS1L166P	PPF	Urethane					#											#			

Table 4B Short-term plasticity: DG.

In vitro									Months of age																				
Paper	Mouse	Observed	Path	Kyn	GB	S/I	Ca	n.s.	1	2	3	4	5	6	7	8	9	10	11	12	13	14	15	16	17	18	≥24
Palop, 2007	hAPPJ20	PPF	MPP	No	P+B	S	2																				
Sun, 2008	hAPPJ20	PPF	LPP	No	Gab	S	2																				
	hAPPJ20/CST3-/-	PPF	LPP	No	Gab	S	2																				
Harris, 2010	hAPPJ20	PPF	MPP	No	P	S	2																				
	D664A	PPF	MPP	No	P	S	2																				
Cissé, 2011	hAPPJ20	PPF	MPP	No	P	S	2																				
	hAPPJ20 with EphB2 lenti	PPF	MPP	No	P	S	2																				
Roberson, 2011	hAPPJ20	PPF	MPP	No	P	S	2																				
	hAPPJ20/Tau-/-	PPF	MPP	No	P	S	2																				
Houeland, 2010	AD11	PPD	MPP	No	P	S	2.5																				
		40 Hz (dep.)	MPP	No	P	S	2.5																				

In vivo					Months of age																		
Paper	Mouse	Observed	Path	Anesthesia	1	2	3	4	5	6	7	8	9	10	11	12	13	14	15	16	17	18	≥24
Matsuyama, 2007	Tg2576	PPF	n.s.	Urethane																			
Huang, 2006	APP23	PPF	n.s.	Sodium penthobarbital																			
Giacchino, 2000	PDAPP/109	PPF	n.s.	Urethane																			#

Results obtained in Tg mice are reported as comparisons against their respective wild-type phenotypes (normal, decrease or increase) through color coding (see top of Table), in an age-dependent manner. Attempts of rescue (in italics in mouse column) are also reported in color codes (see top of Table). Studies are divided into *in vitro* and *in vivo*. The protocol used for the study of short-term plasticity was usually a paired-pulse protocol. In the column 'observed', we report whether the paired-pulse protocol led to facilitation (PPF) or depression (PPD). Note that Houeland (2010) observe PPD at the MPP-granule cell synapse while Palop (2007), Harris (2010), Cissé (2010) and Roberson (2011) observe facilitation at the same MPP synapse (see text for details). Sun (2008) observes PPF at the LPP synapse. Larson (1999) and Houeland (2010) also assessed short-term plasticity using trains of stimuli (at 1, 5, 10 and 40 Hz, respectively), as indicated in this same column. Trains displayed facilitation (fac.) in CA1 and depression (dep.) in DG. For *in vitro* studies, recording conditions are reported: presence of kynurenate (Kyn) during dissection (y: yes); 'GB' indicates the presence of the $GABA_A$ergic blockers, picrotoxin (P) or bicuculline (B), during recordings; 'S/I' refers to recordings in a submerged or interface chamber. The 'Ca' column reports ACSF Ca^{2+} concentration used during experiments. 'n.s.', not specified. For *in vivo* experiments, the anesthesia under which recordings were performed is specified. Experiments done in whole cell configuration are highlighted by bold writing in the 'observed' column. Colored boxes surrounded by black contours highlight direct comparison of a parameter by same experimenter (e.g., for rescue experiments or recording condition). *Electrophysiology performed after behavior; #experimenters report mostly normal PPF except for alterations at a few specific ISIs.

Table 5 Long-term potentiation (LTP) of synaptic transmission at the hippocampal SC-CA1 synapse in AD Tg models.

							Color legend:			Normal			Decrease			Increase			Rescued			Not rescued		
In vitro							Months of age																	
Paper	Mouse	Protocol	Kyn	GB	S/I	Ca^{2+}	n.s.	1	2	3	4	5	6	7	8	9	10	11	12	13	14	15	16	17	18	19-20	≥24
Chapman, 1999	Tg2576	TBS	Yes	No	S	2.5																					
Fitzjohn, 2001	Tg2576	TBS	No	No	S	2.4																					
	Tg2576	TBS	Yes	No	S	2.4																					
Trinchese, 2004	Tg2576	TBS	No	No	n.s.	2			*	*	*	*	*	*	*	*	*	*	*	*							
	Tg2576	TBS	Yes	No	n.s.	2										*	*	*	*	*							
D'Amelio, 2011	Tg2576	HFS, 1×100 Hz	No	P	S	2																					
Roder, 2003	APP23	TBS	No	No	I	2.5																					
Middei, 2010	APP23	HFS, 1×100 Hz	No	No	S	2.4													**								
	APP23	HFS, 1×100 Hz	No	No	S	2.4													*								
Brown, 2005	TAS10	TBS	No	No	I	2																					
Moechars, 1999	APPLd2	HFS, 2×100 Hz (ISI 20 s)	No	No	I	2.4																					
Dewachter, 2002	APPLd2	HFS, 2×100 Hz (ISI 20 s)	No	No	I	2.4																					
Postina, 2004	APPLd2	HFS, 2×100 Hz (ISI 20 s)	No	No	S	n.s.																					
	APPLd2/ ADAM10	HFS, 2×100 Hz (ISI 20 s)	No	No	S	n.s.																					
Dewachter, 2009	APPLd2	n.s.	No	No	I	2.4																					
Hsia, 1999	APPind H6	HFS, 4×100 Hz (ISI 20 s)	No	P	S	2.5																					
Larson, 1999	PDAPP/109	TBS	No	No	I	3.4					#	#															
Hartman, 2005	PDAPP/109	TBS	No	No	S	2.5																		*#	*#	*#	
Dziewczapolski, 2009	hAPPJ9 (PDAPPJ9)	HFS, 4×100 Hz (ISI 5 min)	Yes	No	S	2																					
Saganich, 2006	hAPPJ20	TBS	Yes	No	S	2																					
	D664A	TBS	Yes	No	S	2																					
	hAPPJ20	HFS, 4×100 Hz (ISI 10 s)	Yes	No	S	2																					
	D664A	HFS, 4×100 Hz (ISI 10 s)	Yes	No	S	2																					
Palop, 2007	hAPPJ20	HFS, 4×100 Hz (ISI 20 s)	No	P+B	S	2																					
Harris, 2010	hAPPJ20	HFS, 4×100 Hz (ISI 20 s)	No	No	S	2																					
	D664A	HFS, 4×100 Hz (ISI 20 s)	No	No	S	2																					

Table 5 (Continued)

Color legend: Normal | Decrease | Increase | Rescued | Not rescued

In vitro

Paper	Mouse	Protocol	Kyn	GB	S/I	Ca^{2+}	Months of age: n.s. 1 2 3 4 5 6 7 8 9 10 11 12 13 14 15 16 17 18 19-20 ≥24
Jolas, 2002	TgCRND8	HFS, 1×100 Hz	No	No	S	2.5	
	TgCRND8	TBS	No	No	S	2.5	
	TgCRND8	Weak Burst/ TrainBurst	No	No	S	2.5	
Knobloch, 2007a	ArcBeta	HFS, 3×100 Hz (ISI 20 s)	No	No	I	2.5	
	ArcBeta	*HFS, 3×100 Hz (ISI 20 s)+PP1 inh.*	No	No	I	2.5	
Barrow, 2000	PS1M146L	HFS, 1×100 Hz	No	No	I	2	
Trinchese, 2004	PS1M146L	TBS	No	No	n.s.	2	
Parent, 1999	PS1A246E	HFS, 3×100 Hz (ISI 20 s)	No	No	I	2	
	PS1A246E	TBS	No	No	I	2	
Schneider, 2001	PS1A246E	Weak HFS (0.4 s, 1 Hz)	No	No	n.s.	2.4	
	PS1A246E	HFS, 2×100 Hz (ISI 20 s)	No	No	n.s.	2.4	
Dewachter, 2008	PS1A246E	Weak HFS (0.5 s, 1 Hz)	No	No	n.s.	2.4	
	PS1A246E	HFS, 2×100 Hz (ISI 20 s)	No	No	n.s.	2.4	
Zaman, 2000	PS1ΔE9	HFS, 1×100 Hz	No	No	S	2.5	
	PS1ΔE9	TBS	No	No	S	2.5	
	PS1ΔE9	*TBS+picrotoxin*	No	P	S	2.5	
	PS1ΔE9	*TBS+flunitrazepam*	No	No	S	2.5	
Auffret, 2009	PS1L286V	TBS	No	P	S	2	
Oddo, 2003	PS1M146V KI	HFS, 4×100 Hz (ISI 20 s)	No	No	I	2	
Wang, 2009	PS1M146V KI	HFS, 1×100 Hz	No	P	n.s.	2	
Auffret, 2010	PS1M146V KI	HFS, 1×100 Hz	Yes	P	S	2.5	
		HFS, 4×100 Hz (ISI 5 min) 0–30 min	Yes	P	S	2.5	
		HFS, 4×100 Hz (ISI 5 min) 30 min–3 h	Yes	P	S	2.5	
		HFS, 4×100 Hz (ISI 5 min) 3–4 h	Yes	P	S	2.5	
Trinchese, 2004	APPswe/ PS1M146L	TBS	No	No	n.s.	2	
	APPswe/ PS1M146L	TBS	Yes	No	n.s.	2	

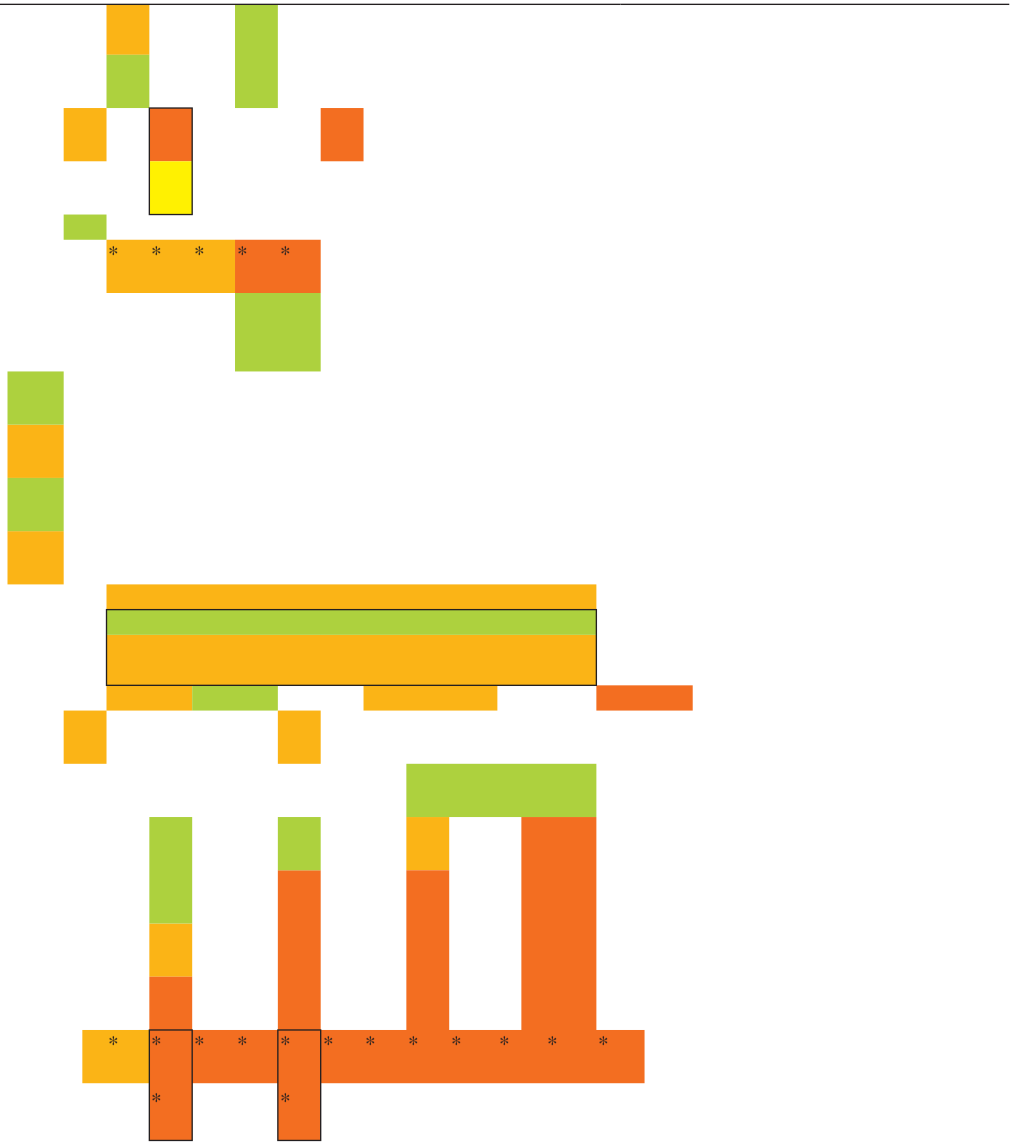

Table 5 (Continued)

Table 5 (Continued)

				Color legend:	Normal	Decrease	Increase	Rescued	Not rescued

In vivo				Months of age																			
Paper	Mouse	Protocol	Anesthesia	n.s.	1	2	3	4	5	6	7	8	9	10	11	12	13	14	15	16	17	18	19-20	≥24
Huang, 2006	APP23	HFS, 4×100 Hz (ISI 10 s)	Sodium penthobarbital																					
Giacchino, 2000	PDAPP/109	HFS, 10×200 Hz (0.75 Hz)	Urethane																					
Gengler, 2010	APPswe/ PS1L166P	HFS, 1×200 Hz	Urethane																					

Results obtained in Tg mice are reported as comparisons against their respective wild-type phenotypes (normal, decrease or increase) through color coding (see top of Table), in an age-dependent manner. Attempts of rescue (in italics in mouse or protocol column) are also reported in color codes (see top of Table; inh., inhibitor). Studies are divided into *in vitro* and *in vivo*. For each study, the protocol of LTP induction is reported. 'TBS' denoted theta-burst stimulation, for which we did not detail the exact protocol used. 'HFS', high frequency stimulation, for which we reported the protocol used. For *in vitro* studies, we report recording conditions: 'Kyn' indicates the presence of kynurenate during the dissection (y: yes; y/n indicates results were the same whether experiments were performed in kynurenate or not); 'GB' indicates the presence of the $GABA_A$ergic blockers, picrotoxin (P) or bicuculline (B), during recordings; 'S/I' refers to recordings in a submerged or interface chamber. The 'Ca' column reports ACSF Ca^{2+} concentration used during experiments. 'n.s.', not specified. In a few cases, electrophysiology experiments were performed after behavior protocols: *, indicates a training protocol; **, indicates pseudo-training; #, indicates that LTP was reduced only at 60 min post-induction, not earlier. For *in vivo* experiments, the anesthesia under which recordings were performed is specified. Colored boxes surrounded by black contours highlight direct comparison of parameter by same experimenter (e.g., for rescue experiments or recording condition).

glutamatergic synaptic strength by insertion of AMPAR at the surface of synapses (Malenka and Bear, 2004). This process is NMDAR- and calcium-dependent. LTP is believed to be a cellular correlate of hippocampal-dependent memory formation and *in vivo* studies suggest that LTP is indeed specifically involved in memory encoding (Gruart et al., 2006; Whitlock et al., 2006). Two types of stimulation protocols are generally used to induce LTP in CA1 pyramidal neurons and DG granule cells. LTP can be elicited by high frequency stimulation (HFS) consisting generally of one of more trains of 100 Hz for 1 s. Increasing the number of trains results in more robust expression of LTP. LTP can also be elicited by theta-bust stimulation (TBS) consisting of a more complex pattern of short high frequency bursts, which are designed to mimic more natural patterns of stimulation. Potentiation of synaptic strength is immediate and is usually analyzed over the next hour, but LTP can last for up to several hours, or even days *in vivo*, depending on the protocol used. Despite the fact that definite proof of causality is still lacking, it is generally believed that loss of LTP underlies memory deficits. It is therefore not surprising that virtually all papers (49/51) evaluating hippocampal function in AD mouse models analyzed LTP. Unfortunately, after over 15 years of evaluation of this parameter, a consensus on whether or not and to what extent LTP is affected in these models is still not reached. All reports of LTP analysis on AD mouse models are summarized in Tables 5 and 6. In these Tables, we have specified the HFS protocol used. Details for TBS protocols, which vary greatly in stimulation pattern between the studies, can be found in the reference papers.

SC-CA1 LTP

Most studies analyzed LTP at the SC-CA1 synapse *in vitro* (39/49). Even with this large body of evidence, a clear-cut conclusion on the functionality of this plasticity in AD models cannot be drawn.

APP-derived models

Studies using APP-derived mouse models provide mixed results with either normal LTP (9/20), impaired LTP (10/20) or increased LTP (1/20) being observed (see Table 5 for references and details). Contrasting data are evident in the Tg2576 and the hAPPJ20 mouse models, where either normal LTP or an age-dependent reduction in LTP are reported for the SC-CA1 synapse (e.g., Chapman et al., 1999 vs. Fitzjohn et al., 2001 or Saganich et al., 2006 vs. Palop et al., 2007). Two other studies of mice also over-expressing hAPPswe, the APP23 and TAS10 models, report normal LTP (Roder et al., 2003; Brown et al., 2005), arguing against a significant effect of over-expression of this transgene on this parameter. Intriguingly, however, Middei et al. (2010) recently reported alterations in LTP only after submitting mice to a behavioral memory task. APP23 mice were submitted to pseudo-training or training in the Morris water maze. Pseudo-trained mice displayed normal LTP, but trained APP23 mice displayed reduced potentiation. These data suggest that challenging the

Table 6 Long-term potentiation (LTP) of synaptic transmission at the hippocampal DG synapse in AD Tg models.

Color legend: Normal | Decrease | Increase | Rescued | Not rescued

In vitro

Paper	Mouse	Protocol	Pathway	Kyn	GB	S/I	Ca	Months of age
Chapman, 1999	Tg2576	TBS	n.s.	Yes	B	S	2.5	
Fitzjohn, 2001	Tg2576	TBS	MPP	Yes	P	S	2.4	
Jacobsen, 2006	Tg2576	TBS	n.s.	No	P	n.s.	n.s.	
Palop, 2007	hAPPJ20	TBS	MPP	No	P+B	S	2	
Sun, 2008	hAPPJ20	TBS (as Palop)	MPP	No	Gab	S	2	
	hAPPJ20/ CST3-/-	TBS (as Palop)	MPP	No	Gab	S	2	
Harris, 2010	hAPPJ20	TBS (as Palop)	MPP	No	P	S	2	
	D664A	TBS (as Palop)	MPP	No	P	S	2	
Cissé, 2011	hAPPJ20	TBS (as Palop)	MPP	No	P	S	2	
	hAPPJ20 with EphB2 lenti	TBS (as Palop)	MPP	No	P	S	2	
Roberson, 2011	hAPPJ20	TBS (as Palop)	MPP	No	P	S	2	
	hAPPJ20/Tau-/-	TBS (as Palop)	MPP	No	P	S	2	
Yoshiike, 2008	APPswe/PS1ΔE9	HFS, 1×100 Hz	n.s.	No	No	n.s.	2	
	APPswe/PS1ΔE9	*HFS, 1×100 Hz+Bic*	n.s	No	B	n.s.	2	
Houeland, 2010	AD11	TBS (as Palop)	MPP	No	P	S	2.5	

In vivo

Paper	Mouse/pathway	Protocol	Pathway	Anesthesia	Months of age
Chapman, 1999	Tg2576	TBS	n.s.	Sodium penthobarbital	
Matsuyama, 2007	Tg2576	HFS, 8×400 Hz	n.s.	Urethane	#
Huang, 2006	APP23	HFS, 1×100 Hz	n.s.	Sodium penthobarbital	
Giacchino, 2000	PDAPP/109	HFS, 10×400 Hz	n.s.	Urethane	
Gureviciene, 2004	APPswe/ PS1A246E	HFS, 6×6×6×400 Hz	n.s.	Awake	* *

Months of age: 1 2 3 4 5 6 7 8 9 10 11 12 13 14 15 16 17 18 ≥24

Results obtained in Tg mice are reported as comparisons against their respective wild-type phenotypes (normal, decrease or increase) through color coding (see top of Table), in an age-dependent manner. Attempts of rescue (in italics in mouse or protocol column) are also reported in color codes (see top of Table). Studies are divided into *in vitro* and *in vivo*. For each study, the protocol of LTP induction is reported. 'Pathway' indicates whether experiments were performed stimulating the medial or the lateral perforant pathway (MPP or LPP). For *in vitro* studies, we report recording conditions: 'Kyn' indicates the presence of kynurenate during the dissection (y: yes); 'GB' indicates the presence of the $GABA_A$ergic blockers, picrotoxin (P), bicuculline (B) or gabazine (Gab), during recordings; 'S/I' refers to recordings in a submerged or interface chamber. The 'Ca' column reports ACSF Ca^{2+} concentration used during experiments. 'n.s.', not specified. For *in vivo* experiments, the anesthesia under which recordings were performed is specified. #, Matsuyama et al. (2007) measured a reduction in population spike; *, reduction is observed only over days and not in the first 60 min. Colored boxes surrounded by black contours highlight direct comparison of parameter by same experimenter (e.g., for rescue experiments or recording condition).

mice with a learning paradigm could facilitate the detection of hippocampal plasticity deficits.

As for *in vitro* data, *in vivo* analysis of LTP in the APP-derived models did not provide clear evidence of a significant LTP impairment (see Table 5 for references and details).

When considering all the reports on APP-derived mice both *in vitro* and *in vivo*, we still cannot reach a clear conclusion on how over-expression of APP mutant transgenes and the resulting Aβ accumulation affect LTP expression at the SC-CA1 synapse. Possible origins of such variability in the results will be discussed later in the review. It is worth noting that these data are in contrast with the current literature demonstrating that acute exposure to synthetic or naturally secreted Aβ impairs hippocampal LTP *in vitro* and *in vivo* (Cullen et al., 1997; Walsh et al., 2002; Wang et al., 2002; Klyubin et al., 2005, 2008; Townsend et al., 2006; Wei et al., 2010).

PS1-derived models

To the best of our knowledge, 10 papers reported LTP analysis of the SC-CA1 synapse in PS1-derived mouse models (see Table 5 for references and details). The picture is clearer than for APP-derived models. Most studies (8/10) report that young adult (1–6 months) transgenic mice over-expressing PS1A246E, PS1M146L, PS1M146V, PS1ΔE9 or PS1L286V display significantly enhanced LTP at the SC-CA1 synapse, especially when induced with a weak protocol (e.g., 1 s or less at 100 Hz), but also with TBS. This phenotype is specific to over-expression of the mutated PS1 protein as mice expressing wild-type PS1 do not display it (Zaman et al., 2000; Dewachter et al., 2008; Auffret et al., 2009). In two longitudinal studies, Auffret et al. (2009, 2010) observed a biphasic phenotype with an enhancement in young mice and a reduction in older mice. This biphasic LTP phenotype is reminiscent of the NMDAR transmission phenotype observed in these mice (Table 2), a correlation that is not surprising since LTP induction is dependent on NMDAR transmission.

In conclusion, although a consensus has not yet been reached, these reports suggest that over-expression of FAD mutant forms of PS1 on LTP positively impacts SC-CA1 LTP expression in the first few months of life, but then impairs it during aging. Analysis of LTP in mice older than 14 months has not been reported, but would help confirm this hypothesis.

APP/PS1 models

Considering the conflicting data obtained in APP-derived mice and the probably biphasic phenotype of PS1-derived mice on SC-CA1 LTP expression, it is not surprising that data obtained in double APP/PS1 transgenics are also controversial (see Table 5 for references and details). Nine publications evaluated SC-CA1 LTP in the various APP/PS1 models with six reporting reduced LTP observed as early as 3 months of age and three reporting normal LTP up to at least 1 year of age. This discrepancy is unlikely to be due to the induction protocol used as both phenotypes were observed using TBS or HFS induction. No conflicting data on the same mouse model have been reported as yet. The type of PS1 mutation harbored by the mice might, however, have influenced the outcome of this analysis as lack of LTP alterations was reported in APPswe/PS1A246E and APPswe/PS1Δ9, while reduced LTP was reported in APPswe/PS1M146L, APPswe/PS1M146V, APPswe/PS1P246L and APPswe/PS1L166P. Finally, an *in vivo* study on APPswe/PS1L166P reports strong impairment of LTP from 8 months of age.

3xTg model

The original study on the 3xTg mouse model reported an impairment of LTP at 6 months of age (Oddo et al., 2003). Wang et al. (2009) could induce robust LTP in 9–12-month-old 3xTg mice. They mention, however, that the LTP observed in these mice is half of that observed in their non-transgenic counterparts, suggesting an LTP impairment, without reporting these data.

AD11 model

We recently reported that both TBS- and HFS-induced SC-CA1 LTPs are normal in AD11 mice at 1 year of age (Houeland et al., 2010), arguing against an effect of NGF-deprivation and correlated AD-like pathology on this type of plasticity.

When summarizing the data obtained in the various AD mouse models, it is currently difficult to draw conclusions on the LTP phenotype at the SC-CA1 synapse. It is likely that this plasticity might be compromised, but only revealed under some experimental conditions and not others. We will discuss the possible impact of methodological variations on these results in the 'variability in methodology' section.

DG LTP

In comparison to SC-CA1 LTP, results of DG LTP analysis are considerably more uniform, but less data are available and fewer types of models have been evaluated than for the SC-CA1 synapse. Ten studies report DG LTP analysis *in vitro*, most of which (9/10) observed a reduction of LTP (see Table 6 for references and details). When specified, the pathway analyzed was always the MPP pathway. So far, only one controversy has emerged regarding the analysis of Tg2576 mice, with two studies reporting reduction of LTP, while one study reports normal LTP. The induction protocols were different in the three reports, but only Fitzjohn et al. (2001) specified the MPP as the pathway analyzed. It is possible that the results vary depending on which pathway is analyzed. All the other studies in the APP-based, and the studies in the APP/PS1 and the AD11 models, report reduced DG LTP with some variability in age of appearance of this deficit. No data are currently available on DG LTP in PS1-derived models. The five *in vivo* studies concerning DG LTP also mostly support an impairment of LTP (4/5) (see Table 6 for references and details).

The available data on the Tg models analyzed therefore support a deficit in LTP in the DG. It will be important to

verify if the deficit is pathway specific and if other AD mouse models that have not yet been analyzed also display this phenotype.

Of the reports that investigated both CA1 and DG LTP in the same mice under the same *in vitro* experimental conditions, Fitzjohn et al. (2001) report normal LTP in both regions, while Chapman et al. (1999), Palop et al. (2007), Harris et al. (2010) and Houeland et al. (2010) report more severe deficits in DG than in CA1, with the last three above-mentioned studies not observing any defects in CA1 at all.

Based on the currently available literature of LTP phenotypes in the different AD mouse models, we can suggest that this plasticity is likely to be more affected in the DG than in the CA1 by the development of AD-like pathology. Understanding why the DG might be more susceptible in the context of AD could provide important new information on the molecular mechanisms of the pathology.

Long-term depression of AMPAR transmission

There are two main forms of long-term depression (LTD) in the hippocampus, both resulting in the weakening of AMPA receptor synaptic transmission. The most studied form of LTD is NMDAR-dependent, but under certain experimental conditions an mGluR-dependent form has also been described (Malenka and Bear, 2004; Luscher and Huber, 2010). Although these two forms of LTD rely on different intracellular mechanisms for induction, they can both be induced by prolonged low frequency stimulation (LFS, typically single or pairs of pulses, 200 ms apart, delivered at 1 Hz for 15 min). This triggers the endocytosis of AMPAR subunits and a long-term reduction in the number of post-synaptic surface AMPARs.

SC-CA1 LTD

LTD has been largely neglected when analyzing hippocampal function in AD mouse models. Only two studies have so far reported LTD analysis (Chang et al., 2006; D'Amelio et al., 2011; see Table 7). Chang et al. (2006), working with the APPNhL/NhL/PS1P246L model, analyzed LTD in an age-dependent study. Using the standard LFS protocol, they report a linear decrease in LTD expression in CA1 pyramidal neurons between 9 and 20 months. By contrast, we recently reported an enhancement of LFS-induced LTD in CA1 pyramidal neurons of early-symptomatic, 3-month-old Tg2576 mice (D'Amelio et al., 2011). These LTD data correlated with enhanced calcineurin-dependent dephosphorylation of the AMPAR subunit GluR1 at Serine 845 (D'Amelio et al., 2011), a molecular process known to occur during NMDAR-dependent LTD (Malenka and Bear, 2004). A longitudinal study on the age-dependency of this alteration needs to be performed to identify its relationship to disease progression.

The only available data therefore demonstrate that LTD of CA1 pyramidal neurons is altered in AD mouse models, but give conflicting results on the nature of this defect. To our knowledge, no studies have reported analysis of LTD in the DG of AD models. It is, however, worthwhile noting that recent studies demonstrate that acute application of Aβ-containing medium on healthy mouse hippocampal slices results in enhanced LTD (Shankar et al., 2008; Li et al., 2009). Furthermore, another study demonstrated that Aβ over-expression in organotypic slices (using viral mediated over-expression of APP) leads to loss of surface AMPAR using mechanisms reminiscent of mGluR-dependent LTD (Hsieh et al., 2006). Considering this literature, it will be important to understand how NMDAR- and mGluR-dependent LTD are affected in the different AD mouse models by in depth analysis of this synaptic parameter and its relationship to disease progression.

Inhibitory GABAergic transmission

Inhibitory GABAergic transmission via local interneurons is essential to brain function, controlling the generation of Na^+- and Ca^{2+}-dependent action potentials, synaptic transmission and plasticity, as well as the generation and pacing of synchronous oscillatory brain activity (Mody and Pearce, 2004; Mann and Paulsen, 2007). Fast, but also tonic, inhibition of excitatory transmission is mediated by ionotropic $GABA_A$ receptors, while G-protein coupled inhibition is mediated by $GABA_B$ metabotropic receptors (Sivilotti and Nistri, 1991; Pinard et al., 2010). The relative diversity of GABAergic interneuron subtypes compared to more uniform pyramidal neurons has rendered electrophysiological studies on these interneurons more difficult. GABAergic transmission onto glutamatergic neurons is generally evaluated by analysis of spontaneous miniature inhibitory post-synaptic currents (sIPSCs), which are generated by action potential-dependent and action potential-independent spontaneous release of GABA quanta from the pre-synaptic terminals. Isolation of action potential-independent miniature IPSCs (mIPSCs) is obtained with the addition of TTX. Evoked IPSCs can also be evaluated by stimulation of local interneurons. Compared to the plethora of papers described above analyzing glutamatergic transmission and plasticity, only a few papers have analyzed hippocampal GABAergic transmission in the CA1, DG and CA3 hippocampal areas of AD mouse models (see Table 8 for references and details).

GABAergic transmission in CA1

Data on CA1 GABAergic function in an APP-derived mouse model TgCNRD8 were obtained from one group (Jolas et al., 2002). An alteration emerges in the properties of IPSCs recorded at 4–5 months of age (see Table 8 for details). A thorough study on CA1 alterations of GABAergic function in 6-month-old AD11 mice was performed by Cherubini's group in two papers. The first study (Rosato-Siri et al., 2006) observed that, contrary to WT mice, nicotine-induced potentiation of glutamatergic function in AD11 mice is dependent on GABA transmission, suggesting that the relationship between cholinergic modulation and inhibitory/excitatory transmission is altered. The follow-up study (Lagostena et al., 2010) demonstrated that GABA was in fact depolarizing and excitatory in this Tg model, a finding supported by single cell data

Table 7 Long-term depression (LTD) of synaptic transmission at the hippocampal SC-CA1 synapse in AD mouse models.

		Color legend:				Normal			Decrease					Increase						
In vitro						Months of age														
Paper	Mouse	Protocol	Kyn	GB	S/I	Ca	1	2	3	4	5	6	7	8	9	10	11	12	13	14–20
D'Amelio, 2011	Tg2576	900 p, 1Hz	No	P	S	4														
Chang, 2006	APPNLh/PS1P246L	Paired 900 p, ISI=200 ms, 1 Hz	Yes	P	S	2														

Results obtained in Tg mice are reported as comparisons against their respective wild-type phenotypes (normal, decrease or increase) through color coding (see top of Table), in an age-dependent manner. All studies were done *in vitro*. The protocol of LTD induction is reported (p=pulses). 'Kyn' indicates the presence of kynurenate during the dissection (y: yes); 'GB' indicates the presence of the $GABA_A$ergic blocker picrotoxin (P) during recordings; 'S/I' refers to recordings in a submerged or interface chamber. The 'Ca' column reports ACSF Ca^{2+} concentration used during experiments.

(impact of GABAergic activity on CA1 pyramidal cell firing, reversal potential of $GABA_A$-mediated post-synaptic currents and of GABA-evoked single-channel currents) as well as by data from extracellular multiple unit activities (MUA) of the CA1 neuronal network. This phenotype was dependent on the serum levels of anti-NGF antibodies and is reminiscent of the action of GABA during early post-natal development.

GABAergic transmission in DG

GABAergic transmission onto DG granule cells was recently studied by Mucke's group (Palop et al., 2007; Roberson et al., 2011) in 3–6-month-old hAPPJ20 mice (see details in Table 8). The authors suggest that inhibitory interneurons make an increased number of effective synapses onto granule cells (as reflected by higher mIPSC frequency), but that the interneurons of transgenic mice are less active (as reflected by lower sIPSC frequency). Additional experiments on sIPSCs in NBQX and APV and analysis of the excitatory/inhibitory balance prompted the authors to further suggest that DG interneurons were less active because of reduced excitatory drive onto them and/or reduced intrinsic excitability. These arguments await further experimental validation by independent investigators and in other models.

GABAergic transmission in CA3

Two studies evaluated GABAergic transmission in CA3 pyramidal neurons (see Table 8 for details and references). Early work by Barrow et al. (2000) of young adult PS1ML146V and PS1ML146L mice failed to detect any alterations in monosynaptic inhibitory post-synaptic potentials (IPSPs) with respect to reversal potential, maximal response amplitude or rise and decay time constants. Analysis of synchronous GABAergic activity in the CA3 of TAS10 mice also argues for normal GABAergic function in this area of the hippocampus (Brown et al., 2005). These first analyses suggest that mutated hAPP or PS1 over-expression does not overtly influence GABAergic function in CA3, but in depth analysis is necessary for confirmation.

We can conclude from the recent studies investigating GABAergic function in some depth in CA1 and DG that the GABAergic system is likely to be significantly affected in these areas of the hippocampus in AD. However, as no thorough longitudinal age-dependent evaluation of these alterations was reported, data interpretation is limited with respect to disease onset and progression. Nevertheless, these data should be taken into consideration when interpreting results obtained while recording glutamatergic transmission and plasticity in the absence of blockers of GABAergic transmission, as will be discussed below.

Variability in methodology

It is clear from the above summaries of the different parameters of hippocampal function assessed in the AD models

Table 8 Basic inhibitory GABAergic synaptic transmission at the hippocampal SC-CA1, DG and CA3 synapses in AD mouse models.

					Color legend:	Normal			Decrease			Increase			Rescued											
In vitro					Months of age																				
Paper	Mouse	Protocol	Kyn	S/I	1	2	3	4	5	6	7	8	9	10	11	12	13	14	15	16	17	18	≥24
Jolas, 2002	TgCRND8	**Normalized eIPCS vs. current stim (I/O) curve**	No	S																			
		eIPSC max amplitude	No	S																			
		eEPSC/eIPCS ratio	No	S																			
		sIPCS freq	No	S																			
		sIPSC amp	No	S																			
Rosato-Siri, 2006	AD11	**Nicotine mediated potentiation of glutamatergic transmission**	No	S						*													
Lagostena, 2010	AD11	**GABA currents**	No	S					**	**													
In vitro																							
Paper	Mouse	Protocol	Kyn	S/I																			
GABAergic transmission MPP-DG																							
Palop, 2007	hAPPJ20	**miniIPSC freq**	No	S																			
		miniIPSC amp (average)	No	S																			
		miniIPSC amp (top 25% only)	No	S																			
Roberson, 2011	hAPPJ20	**miniIPSC freq**	No	S																			
	hAPPJ20/Tau-/-	***miniIPSC freq***	No	S																			
	hAPPJ20	**miniIPSC amp**	No	S																			
	hAPPJ20	**sIPSC freq**	No	S																			
	hAPPJ20/Tau-/-	***sIPSC freq***	No	S																			
	hAPPJ20	**eIPSC amplitude**	No	S																			
	hAPPJ20	**sIPSC/sEPSC**	No	S																			
	hAPPJ20/Tau-/-	***sIPSC/sEPSC***	No	S																			
In-vitro																							
Paper	Mouse	Protocol	Kyn	S/I	1	2	3	4	5	6	7	8	9	10	11	12	13	14	15	16	17	18	≥24
GABAergic transmission: CA3																							
Brown, 2005	TAS10	**ISI of synch GABAergic activity (NBQX+APV)**	No	I																			
Barrow, 2000	PS1M146V	**sIPSP (reversal potential, max amp, kinetics)**	No	I																			
	PS1M146L	**sIPSP (reversal potential, max amp, kinetics)**	No	I																			

Results obtained in Tg mice are reported as comparisons against their respective wild-type phenotypes (normal, decrease or increase) through color coding (see top of Table), in an age-dependent manner. Attempts of rescue (in italics in mouse or protocol column) are also reported in color codes (see top of Table). All studies are done *in vitro* and are divided by type of synapse (SC-CA1 or MPP-DG and CA3). The protocol through which GABAergic function was assessed is reported: ISI, inter-stimulus interval; freq, frequency; amp, amplitude; eIPSC, evoked IPSC; sIPSC, spontaneous IPSC. None of the studies added kynurenic (Kyn) acid during the dissection. Submerged (S) vs. interface (I) recording conditions is specified. *, Nicotine normally induces a potentiation of glutamatergic transmission independent of GABA transmission, but in AD11 mice this potentiation becomes GABA dependent as it does not occur in the presence of bicuculline. **, GABA becomes depolarizing in AD11 mice. Colored boxes surrounded by black contours highlight direct comparison of parameter by same experimenter (e.g., for rescue experiments).

that investigators have consistently run into conflicting data. These discrepancies are as yet mostly unexplained but could stem from use of different mouse models which display different levels of transgene expression and/or different levels of APP proteolysis. However, these above-mentioned possible explanations cannot account for conflicting data obtained in identical mouse models. In this section, we therefore discuss what we believe could be possible methodological variabilities at the basis of conflicting data.

Kynurenic acid

The excitotoxicity that inevitably occurs during dissection can lead to highly variable health of slices. This has led to the hypothesis that transgenic vs. wild-type mice could be differentially affected by the slicing process. The difference could trigger the appearance of deficits in synaptic transmission of Tgs that were not present in the intact animal (as proposed by Hsia et al., 1999) or allow detection of subtle defects that are exacerbated by the dissection itself (Fitzjohn et al., 2001). Several groups used the broad spectrum excitatory amino acid receptor antagonist kynurenic acid during the dissection to reduce excitotoxicity (see Tables 2–8), but the comparison with studies that did not use kynurenic acid could be influenced by other methodological differences. We could find four papers that use both conditions (presence or not of kynurenic acid) within the same study, making it easier to draw conclusions. Fitzjohn et al. (2001) demonstrated that a reduction in synaptic transmission can be avoided at 12 months of age, but not at 18 months, in Tg2576 mice by addition of kynurenic acid during dissection (see Table 2), suggesting that kynurenic acid addition might prevent detection of subtle synaptic defects, which become more pronounced with age. The other three studies (Hsia et al., 1999; Gong et al., 2004; Trinchese et al., 2004), however, reported that addition of kynurenic acid during the dissection did not prevent the impairments in basic transmission and LTP they observed (see Table 2).

In general, as there is no standard universal procedure for slice dissection (for example, addition of kynurenic acid, sucrose, ascorbic acid during the dissection, and conditions of recovery such as time, temperature, interface vs. submerged, etc.), it cannot be excluded that dissection procedures influence the outcome of the recordings. Until discrepancies are resolved, we advocate that the methodological details of this procedure should be well documented in publications for future investigators to be able to reproduce the data.

Strain background

There is a large variability in the background used to generate the mouse models, but in the past few years investigators have tried to backcross to C57BL6 mice whenever possible. It is also possible that subtle differences in background arise from in-house breeding of the species. Trinchese et al. (2004) report differences in the likelihood of finding good and consistent responses depending on the mouse strain used. In particular, they report that single transgenic Tg2576 mice give higher variability in this sense than double transgenic APPswe/PS1M146L. As differences in electrophysiological properties of different mouse strains have been reported in the past (Nguyen et al., 2000), a different susceptibility to excitotoxicity of Tg2576 mice (C57Bl6/SJL hybrid background) vs. APPswe/PS1M146L mice (PS1:SW/B6D2 background) is not to be excluded.

Activity-dependent changes in Aβ levels

In vitro studies demonstrated that synaptic activation influences the levels of both extracellular and intraneuronal Aβ (Kamenetz et al., 2003; Tampellini et al., 2009) and that it can protect against Aβ-related synaptic changes (Tampellini et al., 2009). These *in vitro* observations are strengthened by the report that synaptic activity rapidly and directly influences the level of Aβ in the interstitial fluid *in vivo* (Cirrito et al., 2005). While these are interesting observations in view of therapeutic strategies for AD patients, changes in brain activity levels in animals housed in different laboratories or possibly even variations in hippocampal slice activity due to different slicing and recording conditions (e.g., use of receptor blockers) could be a cause of conflicting results observed.

Use of $GABA_A$ blockers

Most investigators evaluating glutamatergic transmission and plasticity did not include blockers of GABAergic transmission (see Tables 2–6). Some investigators use these blockers for recording DG LTP but not CA1 LTP. We suggest that this omission should be taken into account when interpreting data. Indeed, GABAergic transmission is known to regulate excitatory transmission and plasticity of principal glutamatergic neurons via fast stimulation-dependent and tonic activation of $GABA_A$ receptors (Wigstrom and Gustafsson, 1986; Evans and Viola-McCabe, 1996; Seabrook et al., 1997) and the few studies reporting analysis of GABAergic transmission in AD mouse models suggest significant alterations of the GABAergic system, as detailed above. In fact, two studies report that inclusion of GABA blockers impacted the synaptic plasticity phenotype of the AD mouse model under study (Zaman et al., 2000; Yoshiike et al., 2008; see Tables 5 and 6 for details). These data demonstrate that the balance between excitation and inhibition is likely to be perturbed in AD as suggested by Palop and Mucke (2010), and therefore evaluation of glutamatergic function would be more accurately interpreted in conditions where GABAergic transmission is blocked and *vice versa*.

Calcium concentration in the external medium

As detailed in the basic synaptic transmission section, we have recently observed that lowering external calcium to 1 mM revealed synaptic transmission deficits in AD11 mice not observed at the standard concentration of 2.5 mM (Houeland et al., 2010). Virtually all investigators have analyzed synaptic function of AD models in variable calcium concentration ranging from 2 to 3.5 mM (see Tables 2–7), although calcium

concentration in the CSF *in vivo* ranges between 1 and 2 mM, decreasing with age (Jones and Keep, 1988). Also, it is becoming increasingly clear that Aβ pathogenicity is tightly linked to neuronal calcium signaling (Demuro et al., 2010). It is therefore possible that disparity in the calcium concentrations used in the various studies influenced the results. Furthermore, analyzing synaptic function in conditions of lowered release probability might permit the detection of as yet uncharacterized phenotypes.

Rescue experiments

The use of AD models has enabled investigators to assess the importance of specific proteins or the potential of pharmacological compounds in the rescue of observed phenotypes. In this section, we will briefly summarize the different publications that described the rescue of hippocampal plasticity phenotypes. These rescue experiments are detailed in Tables 2–8.

Rescue by rolipram

Rolipram is a specific inhibitor of the phosphodiesterase type 4 (PDE4) isoform which enhances signaling through cAMP, including activation of PKA/transcription factor cAMP Response Element Binding protein (CREB) pathway. Gong et al. (2004) described rescue of basic synaptic transmission and LTP at the SC-CA1 synapse in APPswe/PS1M146L mice after chronic intraperitoneal treatment with rolipram. They further demonstrate that this treatment rescues the levels of phosphorylated CREB, which were lower in untreated APPswe/PS1M146L mice. These data suggest that enhancing activation of the cAMP/PKA/CREB pathway might be beneficial in restoring normal hippocampal function, although evidence of the direct involvement of CREB is lacking as cAMP and PKA are known to also target other substrates.

Rescue by over-expression of ADAM10

ADAM10 is a disintegrin and metalloproteinase that can cleave APP at the main α-secretase site thus augmenting the non-amyloidogenic processing of APP. Over-expression of ADAM10 in a mouse that also expresses the APPLond mutation (APP/Ld/ADAM10 mouse) rescued the LTP impairment observed in the APP/Ld single mutant (Postina et al., 2004). These data suggest that favoring the non-amyloidogenic processing of APP could be a beneficial strategy to restore normal hippocampal function.

Cleavage of APP at D664

APP contains a consensus site for caspase cleavage at D664 resulting in the generation of the intracellular C31 fragment. To understand the importance of this cleavage in impairment of hippocampal function, D664A mice were created by introduction of the D664A mutation in the APPswe/ind transgene (as expressed in the hAPPJ20 line), thus preventing caspase cleavage (Galvan et al., 2006). Two studies analyzed these mice by electrophysiology and reported conflicting results. Saganich et al. (2006) report that introduction of the D664A mutation rescues basic synaptic transmission and LTP at the SC-CA1 synapse, which they observed in hAPPJ20. In contrast, Harris et al. (2010) did not observe any rescue of SC-CA1 basic synaptic transmission and of the MPP-DG LTP phenotype that they had previously characterized in the hAPPJ20 mice. At present, we cannot therefore conclude on the importance of this caspase cleavage site in relation to impairments of hippocampal function.

Rescue by genetic ablation of Cystatin C gene

Cystatin C (Cys3) is a protease that inhibits Cathepsin B (CatB), an Aβ degrading enzyme. Inhibition of Cys3 results in enhanced activity of CatB and thus enhanced degradation of Aβ. Sun et al. (2008) crossed hAPPJ20 mice with Cys3 null mice ($Cys3^{-/-}$) to evaluate if loss of Cys3 could rescue hippocampal function. They report that hAPPJ20/$Cys3^{-/-}$ mice still displayed reduced basic synaptic transmission at the SC-CA1 synapse. Deletion of Cys3, however, rescued the PPR ratio at the LPP-DG synapse and rescued LTP at the MPP-DG synapse. These data suggest that inhibition of Cys3 protease activity could be a potential therapeutic target for AD.

Rescue by genetic ablation of α7 nicotinic acetylcholine receptor (α7nAChR) gene

Aβ42 was shown to bind to the α7nAChR with high affinity and both are found colocalized in neuritic plaques of human AD brains (Wang et al., 2000a,b). Dziewczapolski et al. (2009) therefore evaluated the impact of deleting the α7nAChR gene on hippocampal function of hAPPJ9 mice. The impairment they observed in hAPPJ9 mice was partially rescued in hAPPJ9/α7nAChR -/- double transgenic mice, suggesting that inhibition of α7nAChR function could be beneficial in the treatment of AD.

Rescue by Aβ antibodies

One therapeutic approach that has received a lot of attention in the last decade is the use of immunization against Aβ to interfere with its deposition and speed up its clearance (Golde et al., 2011). Knobloch et al. (2007a) report that a single dose of intraperitoneal injection of an antibody (6E10) directed against the Aβ sequence was sufficient to reverse the LTP deficit they observed in ArcAβ mice. We could not find other electrophysiological evaluations of the effects of Aβ immunization on hippocampal function in AD mouse models. This paucity of data is surprising considering the large body of literature assessing the benefits of this type of immunization in AD models (see Wisniewski and Sigurdsson, 2010 for review).

Rescue by inhibition of protein phosphatase 1

Protein phosphatase 1 (PP1) is known to be involved in the regulation of NMDAR-dependent synaptic plasticity by dephosphorylating key synaptic proteins (Munton et al., 2004). Knobloch et al. (2007a) demonstrated that blocking its activity acutely by bathing slices of ArcAβ or APPswe/

PS1M146L mice in the selective inhibitor tautomycin rescued the LTP impairments observed at the SC-CA1 synapse. These data suggest that PP1 is implicated in this impairment and that its inhibition could restore normal plasticity.

Rescue by inhibition of calpains

Calpains are calcium-dependent proteases, the activity of which is abnormally elevated in AD (Trinchese et al., 2008 and references therein). Trinchese et al. (2008) showed that pharmacologically inhibiting calpain activity restored synaptic transmission and LTP in the APPswe/PS1M146L mouse model. These data suggest that calpain inhibition may prove useful as a therapeutic target.

Rescue by increasing expression of X11β

X11β is a neuronal adaptor protein that binds to the intracellular domain of APP (Mitchell et al., 2009 and references therein). Alterations to X11β expression influence APP processing and Aβ production. Mitchell et al. (2009) crossed X11β over-expressing mice with Tg2576 mice and demonstrated by *in vivo* electrophysiology that this manipulation rescued the late phase LTP impairments they observed in the Tg2576 mice. These data suggest that modulating X11β function could be beneficial in AD.

Rescue by increase in EphB2 expression

EphB2 is a receptor tyrosine kinase that regulates NMDAR trafficking and function. It is implicated in the regulation of NMDAR-dependent Ca^{2+} influx and down-stream activation of transcription factors that mediate synaptic plasticity. Cissé et al. (2011) injected a lentivirus expressing EphB2 in the CA1 or DG of hAPPJ20 mice. They report that increased expression of EphB2 is sufficient to rescue NMDAR transmission and LTP, parameters that were reduced at the MPP-DG synapse in hAPPJ20 mice, but not sufficient to rescue the lower PPR at the MPP-synapse nor the basic synaptic transmission deficit observed at the SC-CA1 synapse. The authors conclude that increasing EphB2 levels could be beneficial in AD.

Rescue by inhibition of caspase 3

We recently reported that acutely treating hippocampal slices of Tg2576 mice with the caspase 3 inhibitor z-DEVD-*fmk* is sufficient to restore normal AMPAR/NMDAR ratios at the SC-CA1 synapse (D'Amelio et al., 2011). These data suggest that increased activation of caspase 3 is responsible for disrupting the balance between AMPAR and NMDAR transmission at this synapse and that inhibiting its activity could be sufficient to restore normal synaptic balance.

Rescue by removal of tau

Several studies suggest that the microtubule-associated protein tau mediates or enables the pathogenic effects of Aβ (Ittner and Gotz, 2011). Roberson et al. (2011) therefore evaluated the effects of removing tau on hippocampal synaptic function by crossing hAPPJ20 mice with tau-/- mice. Removing tau restored all excitatory and inhibitory transmission and plasticity deficits that they had observed in hAPPJ20. These data suggest that tau is a key protein mediating hippocampal functional deficits in these mice and that lowering its expression could be beneficial in AD.

These various studies provide important information on the potential therapeutic targets to be considered to restore normal hippocampal function. Their interpretation is, however, still limited as no independent studies are yet available to confirm or challenge these findings, except for the D664A mice where conflicting data have emerged. It will therefore be important to test these rescue approaches in other mouse models.

Future perspectives

Several approaches could help make sense of how hippocampal function is perturbed during AD-like neurodegeneration. First, we advocate dissociation of analysis of GABAergic and glutamatergic function by systematic use of blockers. Also, to understand how the different parameters of hippocampal function are affected with disease progression, we suggest a more systematic age-dependent analysis of the phenotype observed. Finally, to identify the alterations of hippocampal function that are more likely to contribute to AD-related memory loss, we propose the concept of common denominators (Houeland et al., 2010). The common denominators to the most comprehensive AD mouse models, independent of their etiology, are accumulation of Aβ, tau hyperphosphorylation and memory deficits. By comparing the data on hippocampal function in the various models as summarized in this review, we believe that, at present, impairment of DG plasticity and alterations of GABAergic function could be two other common denominators responsible for memory loss, irrespective of the origin of the insult (e.g., mutant hAPP over-expression or loss of NGF trophic support). Further analysis of these hippocampal parameters in other mouse models is necessary to support or challenge this notion, but this type of approach could prove useful for the development of targeted therapeutic strategies. Finally, we found that some crucial aspects of hippocampal synaptic function, such as LTD or CA3 transmission and plasticity, have been almost, if not completely, ignored. Analysis of novel aspects of hippocampal physiology in the models will help to understand how this structure is affected during AD-like neurodegeneration.

Acknowledgements

Although we have made a thorough and extensive search of the literature, we apologize to our colleagues if we mistakenly excluded their studies from our analysis. Figure 1 was designed by Frank Aguilera (IPMC, France). We thank Dr. Lanté, Dr. Houeland and Dr. Checler for critical reading of the manuscript and helpful discussions.

References

Abramov, E., Dolev, I., Fogel, H., Ciccotosto, G.D., Ruff, E., and Slutsky, I. (2009). Amyloid-beta as a positive endogenous regulator of release probability at hippocampal synapses. Nat. Neurosci. *12*, 1567–1576.

Ashe, K.H. and Zahs, K.R. (2010). Probing the biology of Alzheimer's disease in mice. Neuron *66*, 631–645.

Auffret, A., Gautheron, V., Repici, M., Kraftsik, R., Mount, H.T., Mariani, J., and Rovira, C. (2009). Age-dependent impairment of spine morphology and synaptic plasticity in hippocampal CA1 neurons of a presenilin 1 transgenic mouse model of Alzheimer's disease. J. Neurosci. *29*, 10144–10152.

Auffret, A., Gautheron, V., Mattson, M.P., Mariani, J., and Rovira, C. (2010). Progressive age-related impairment of the late long-term potentiation in Alzheimer's disease presenilin-1 mutant knock-in mice. J. Alzheimers Dis. *19*, 1021–1033.

Barrow, P.A., Empson, R.M., Gladwell, S.J., Anderson, C.M., Killick, R., Yu, X., Jefferys, J.G., and Duff, K. (2000). Functional phenotype in transgenic mice expressing mutant human presenilin-1. Neurobiol. Dis. *7*, 119–126.

Bittner, T., Fuhrmann, M., Burgold, S., Ochs, S.M., Hoffmann, N., Mitteregger, G., Kretzschmar, H., LaFerla, F.M., and Herms, J. (2010). Multiple events lead to dendritic spine loss in triple transgenic Alzheimer's disease mice. PLoS One *5*, e15477.

Borchelt, D.R., Thinakaran, G., Eckman, C.B., Lee, M.K., Davenport, F., Ratovitsky, T., Prada, C.M., Kim, G., Seekins, S., Yager, D., et al. (1996). Familial Alzheimer's disease-linked presenilin 1 variants elevate Abeta1-42/1-40 ratio *in vitro* and *in vivo*. Neuron *17*, 1005–1013.

Brown, J.T., Richardson, J.C., Collingridge, G.L., Randall, A.D., and Davies, C.H. (2005). Synaptic transmission and synchronous activity is disrupted in hippocampal slices taken from aged TAS10 mice. Hippocampus *15*, 110–117.

Calella, A.M., Farinelli, M., Nuvolone, M., Mirante, O., Moos, R., Falsig, J., Mansuy, I.M., and Aguzzi, A. (2010). Prion protein and Aβ-related synaptic toxicity impairment. EMBO Mol. Med. *2*, 306–314.

Capsoni, S. and Cattaneo, A. (2006). On the molecular basis linking nerve growth factor (NGF) to Alzheimer's disease. Cell Mol. Neurobiol. *26*, 619–633.

Capsoni, S., Ugolini, G., Comparini, A., Ruberti, F., Berardi, N., and Cattaneo, A. (2000). Alzheimer-like neurodegeneration in aged antinerve growth factor transgenic mice. Proc. Natl. Acad. Sci. USA *97*, 6826–6831.

Chang, E.H., Savage, M.J., Flood, D.G., Thomas, J.M., Levy, R.B., Mahadomrongkul, V., Shirao, T., Aoki, C., and Huerta, P.T. (2006). AMPA receptor downscaling at the onset of Alzheimer's disease pathology in double knockin mice. Proc. Natl. Acad. Sci. USA *103*, 3410–3415.

Chapman, P.F., White, G.L., Jones, M.W., Cooper-Blacketer, D., Marshall, V.J., Irizarry, M., Younkin, L., Good, M.A., Bliss, T.V., Hyman, B.T., et al. (1999). Impaired synaptic plasticity and learning in aged amyloid precursor protein transgenic mice. Nat. Neurosci. *2*, 271–276.

Chishti, M.A., Yang, D.S., Janus, C., Phinney, A.L., Horne, P., Pearson, J., Strome, R., Zuker, N., Loukides, J., French, J., et al. (2001). Early-onset amyloid deposition and cognitive deficits in transgenic mice expressing a double mutant form of amyloid precursor protein 695. J. Biol. Chem. *276*, 21562–21570.

Cirrito, J.R., Yamada, K.A., Finn, M.B., Sloviter, R.S., Bales, K.R., May, P.C., Schoepp, D.D., Paul, S.M., Mennerick, S., and Holtzman, D.M. (2005). Synaptic activity regulates interstitial fluid amyloid-β levels *in vivo*. Neuron *48*, 913–922.

Cissé, M., Halabisky, B., Harris, J., Devidze, N., Dubal, D.B., Sun, B., Orr, A., Lotz, G., Kim, D.H., Hamto, P., et al. (2011). Reversing EphB2 depletion rescues cognitive functions in Alzheimer model. Nature *469*, 47–52.

Citron, M., Westaway, D., Xia, W., Carlson, G., Diehl, T., Levesque, G., Johnson-Wood, K., Lee, M., Seubert, P., Davis, A., et al. (1997). Mutant presenilins of Alzheimer's disease increase production of 42-residue amyloid β-protein in both transfected cells and transgenic mice. Nat. Med. *3*, 67–72.

Colino, A. and Malenka, R.C. (1993). Mechanisms underlying induction of long-term potentiation in rat medial and lateral perforant paths *in vitro*. J. Neurophysiol. *69*, 1150–1159.

Cullen, W.K., Suh, Y.H., Anwyl, R., and Rowan, M.J. (1997). Block of LTP in rat hippocampus *in vivo* by β-amyloid precursor protein fragments. Neuroreport *8*, 3213–3217.

D'Amelio, M., Cavallucci, V., Middei, S., Marchetti, C., Pacioni, S., Ferri, A., Diamantini, A., De Zio, D., Carrara, P., Battistini, L., et al. (2011). Caspase-3 triggers early synaptic dysfunction in a mouse model of Alzheimer's disease. Nat. Neurosci. *14*, 69–76.

Demuro, A., Parker, I., and Stutzmann, G.E. (2010). Calcium signaling and amyloid toxicity in Alzheimer disease. J. Biol. Chem. *285*, 12463–12468.

Dewachter, I., Reverse, D., Caluwaerts, N., Ris, L., Kuiperi, C., Van den Haute, C., Spittaels, K., Umans, L., Serneels, L., Thiry, E., et al. (2002). Neuronal deficiency of presenilin 1 inhibits amyloid plaque formation and corrects hippocampal long-term potentiation but not a cognitive defect of amyloid precursor protein [V717I] transgenic mice. J. Neurosci. *22*, 3445–3453.

Dewachter, I., Ris, L., Croes, S., Borghgraef, P., Devijver, H., Voets, T., Nilius, B., Godaux, E., and Van Leuven, F. (2008). Modulation of synaptic plasticity and Tau phosphorylation by wild-type and mutant presenilin 1. Neurobiol. Aging *29*, 639–652.

Dewachter, I., Filipkowski, R.K., Priller, C., Ris, L., Neyton, J., Croes, S., Terwel, D., Gysemans, M., Devijver, H., Borghgraef, P., et al. (2009). Deregulation of NMDA-receptor function and down-stream signaling in APP[V717I] transgenic mice. Neurobiol. Aging *30*, 241–256.

Duff, K., Eckman, C., Zehr, C., Yu, X., Prada, C.M., Perez-tur, J., Hutton, M., Buee, L., Harigaya, Y., Yager, D., et al. (1996). Increased amyloid-β42(43) in brains of mice expressing mutant presenilin 1. Nature *383*, 710–713.

Dziewczapolski, G., Glogowski, C.M., Masliah, E., and Heinemann, S.F. (2009). Deletion of the α7 nicotinic acetylcholine receptor gene improves cognitive deficits and synaptic pathology in a mouse model of Alzheimer's disease. J. Neurosci. *29*, 8805–8815.

Elder, G.A., Gama Sosa, M.A., and De Gasperi, R. (2010). Transgenic mouse models of Alzheimer's disease. Mt. Sinai J. Med. *77*, 69–81.

Evans, M.S. and Viola-McCabe, K.E. (1996). Midazolam inhibits long-term potentiation through modulation of GABAA receptors. Neuropharmacology *35*, 347–357.

Fitzjohn, S.M., Morton, R.A., Kuenzi, F., Rosahl, T.W., Shearman, M., Lewis, H., Smith, D., Reynolds, D.S., Davies, C.H., Collingridge, G.L., et al. (2001). Age-related impairment of synaptic transmission but normal long-term potentiation in transgenic mice that overexpress the human APP695SWE mutant form of amyloid precursor protein. J. Neurosci. *21*, 4691–4698.

Fitzjohn, S.M., Kuenzi, F., Morton, R.A., Rosahl, T.W., Lewis, H., Smith, D., Seabrook, G.R., and Collingridge, G.L. (2010). A study of long-term potentiation in transgenic mice over-expressing mutant forms of both amyloid precursor protein and presenilin-1. Mol. Brain *3*, 21.

Flood, D.G., Reaume, A.G., Dorfman, K.S., Lin, Y.G., Lang, D.M., Trusko, S.P., Savage, M.J., Annaert, W.G., De Strooper, B., Siman, R., et al. (2002). FAD mutant PS-1 gene-targeted mice: increased Aβ 42 and Aβ deposition without APP overproduction. Neurobiol. Aging *23*, 335–348.

Galvan, V., Gorostiza, O.F., Banwait, S., Ataie, M., Logvinova, A.V., Sitaraman, S., Carlson, E., Sagi, S.A., Chevallier, N., Jin, K., et al. (2006). Reversal of Alzheimer's-like pathology and behavior in human APP transgenic mice by mutation of Asp664. Proc. Natl. Acad. Sci. USA *103*, 7130–7135.

Games, D., Adams, D., Alessandrini, R., Barbour, R., Berthelette, P., Blackwell, C., Carr, T., Clemens, J., Donaldson, T., Gillespie, F., et al. (1995). Alzheimer-type neuropathology in transgenic mice overexpressing V717F β-amyloid precursor protein. Nature *373*, 523–527.

Games, D., Buttini, M., Kobayashi, D., Schenk, D., and Seubert, P. (2006). Mice as models: transgenic approaches and Alzheimer's disease. J. Alzheimers Dis. *9*, 133–149.

Gengler, S., Hamilton, A., and Holscher, C. (2010). Synaptic plasticity in the hippocampus of a APP/PS1 mouse model of Alzheimer's disease is impaired in old but not young mice. PLoS One *5*, e9764.

Giacchino, J., Criado, J.R., Games, D., and Henriksen, S. (2000). *In vivo* synaptic transmission in young and aged amyloid precursor protein transgenic mice. Brain Res. *876*, 185–190.

Golde, T.E., Schneider, L.S., and Koo, E.H. (2011). Anti-Aβ therapeutics in Alzheimer's disease: the need for a paradigm shift. Neuron *69*, 203–213.

Gong, B., Vitolo, O.V., Trinchese, F., Liu, S., Shelanski, M., and Arancio, O. (2004). Persistent improvement in synaptic and cognitive functions in an Alzheimer mouse model after rolipram treatment. J. Clin. Invest. *114*, 1624–1634.

Gruart, A., Munoz, M.D., and Delgado-Garcia, J.M. (2006). Involvement of the CA3-CA1 synapse in the acquisition of associative learning in behaving mice. J. Neurosci. *26*, 1077–1087.

Guo, Q., Fu, W., Sopher, B.L., Miller, M.W., Ware, C.B., Martin, G.M., and Mattson, M.P. (1999). Increased vulnerability of hippocampal neurons to excitotoxic necrosis in presenilin-1 mutant knock-in mice. Nat. Med. *5*, 101–106.

Gureviciene, I., Ikonen, S., Gurevicius, K., Sarkaki, A., van Groen, T., Pussinen, R., Ylinen, A., and Tanila, H. (2004). Normal induction but accelerated decay of LTP in APP+ PS1 transgenic mice. Neurobiol. Dis. *15*, 188–195.

Harris, J.A., Devidze, N., Halabisky, B., Lo, I., Thwin, M.T., Yu, G.Q., Bredesen, D.E., Masliah, E., and Mucke, L. (2010). Many neuronal and behavioral impairments in transgenic mouse models of Alzheimer's disease are independent of caspase cleavage of the amyloid precursor protein. J. Neurosci. *30*, 372–381.

Hartman, R.E., Izumi, Y., Bales, K.R., Paul, S.M., Wozniak, D.F., and Holtzman, D.M. (2005). Treatment with an amyloid-β antibody ameliorates plaque load, learning deficits, and hippocampal long-term potentiation in a mouse model of Alzheimer's disease. J. Neurosci. *25*, 6213–6220.

Houeland, G., Romani, A., Marchetti, C., Amato, G., Capsoni, S., Cattaneo, A., and Marie, H. (2010). Transgenic mice with chronic NGF deprivation and Alzheimer's disease-like pathology display hippocampal region-specific impairments in short- and long-term plasticities. J. Neurosci. *30*, 13089–13094.

Hsia, A.Y., Masliah, E., McConlogue, L., Yu, G.Q., Tatsuno, G., Hu, K., Kholodenko, D., Malenka, R.C., Nicoll, R.A., and Mucke, L. (1999). Plaque-independent disruption of neural circuits in Alzheimer's disease mouse models. Proc. Natl. Acad. Sci. USA *96*, 3228–3233.

Hsiao, K., Chapman, P., Nilsen, S., Eckman, C., Harigaya, Y., Younkin, S., Yang, F., and Cole, G. (1996). Correlative memory deficits, Aβ elevation, and amyloid plaques in transgenic mice. Science *274*, 99–102.

Hsieh, H., Boehm, J., Sato, C., Iwatsubo, T., Tomita, T., Sisodia, S., and Malinow, R. (2006). AMPAR removal underlies Aβ-induced synaptic depression and dendritic spine loss. Neuron *52*, 831–843.

Huang, S.M., Mouri, A., Kokubo, H., Nakajima, R., Suemoto, T., Higuchi, M., Staufenbiel, M., Noda, Y., Yamaguchi, H., Nabeshima, T., et al. (2006). Neprilysin-sensitive synapse-associated amyloid-β peptide oligomers impair neuronal plasticity and cognitive function. J. Biol. Chem. *281*, 17941–17951.

Ittner, L.M. and Gotz, J. (2011). Amyloid-β and tau – a toxic pas de deux in Alzheimer's disease. Nat. Rev. Neurosci. *12*, 65–72.

Jacobsen, J.S., Wu, C.C., Redwine, J.M., Comery, T.A., Arias, R., Bowlby, M., Martone, R., Morrison, J.H., Pangalos, M.N., Reinhart, P.H., et al. (2006). Early-onset behavioral and synaptic deficits in a mouse model of Alzheimer's disease. Proc. Natl. Acad. Sci. USA *103*, 5161–5166.

Jankowsky, J.L., Xu, G., Fromholt, D., Gonzales, V., and Borchelt, D.R. (2003). Environmental enrichment exacerbates amyloid plaque formation in a transgenic mouse model of Alzheimer disease. J. Neuropathol. Exp. Neurol. *62*, 1220–1227.

Jolas, T., Zhang, X.S., Zhang, Q., Wong, G., Del Vecchio, R., Gold, L., and Priestley, T. (2002). Long-term potentiation is increased in the CA1 area of the hippocampus of APP(swe/ind) CRND8 mice. Neurobiol. Dis. *11*, 394–409.

Jones, H.C. and Keep, R.F. (1988). Brain fluid calcium concentration and response to acute hypercalcaemia during development in the rat. J. Physiol. *402*, 579–593.

Kamenetz, F., Tomita, T., Hsieh, H., Seabrook, G., Borchelt, D., Iwatsubo, T., Sisodia, S., and Malinow, R. (2003). APP processing and synaptic function. Neuron *37*, 925–937.

Karow, D.S., McEvoy, L.K., Fennema-Notestine, C., Hagler, D.J. Jr., Jennings, R.G., Brewer, J.B., Hoh, C.K., and Dale, A.M. (2010). Relative capability of MR imaging and FDG PET to depict changes associated with prodromal and early Alzheimer disease. Radiology *256*, 932–942.

Kesner, R.P. and Hopkins, R.O. (2006). Mnemonic functions of the hippocampus: a comparison between animals and humans. Biol. Psychol. *73*, 3–18.

Klyubin, I., Walsh, D.M., Lemere, C.A., Cullen, W.K., Shankar, G.M., Betts, V., Spooner, E.T., Jiang, L., Anwyl, R., Selkoe, D.J., et al. (2005). Amyloid β protein immunotherapy neutralizes Aβ oligomers that disrupt synaptic plasticity *in vivo*. Nat. Med. *11*, 556–561.

Klyubin, I., Betts, V., Welzel, A.T., Blennow, K., Zetterberg, H., Wallin, A., Lemere, C.A., Cullen, W.K., Peng, Y., Wisniewski, T., et al. (2008). Amyloid β protein dimer-containing human CSF disrupts synaptic plasticity: prevention by systemic passive immunization. J. Neurosci. *28*, 4231–4237.

Knobloch, M., Farinelli, M., Konietzko, U., Nitsch, R.M., and Mansuy, I.M. (2007a). Abeta oligomer-mediated long-term potentiation impairment involves protein phosphatase 1-dependent mechanisms. J. Neurosci. *27*, 7648–7653.

Knobloch, M., Konietzko, U., Krebs, D.C., and Nitsch, R.M. (2007b). Intracellular Abeta and cognitive deficits precede β-amyloid

deposition in transgenic arcAβ mice. Neurobiol. Aging *28*, 1297–1306.

Lagostena, L., Rosato-Siri, M., D'Onofrio, M., Brandi, R., Arisi, I., Capsoni, S., Franzot, J., Cattaneo, A., and Cherubini, E. (2010). In the adult hippocampus, chronic nerve growth factor deprivation shifts GABAergic signaling from the hyperpolarizing to the depolarizing direction. J. Neurosci. *30*, 885–893.

Larson, J., Lynch, G., Games, D., and Seubert, P. (1999). Alterations in synaptic transmission and long-term potentiation in hippocampal slices from young and aged PDAPP mice. Brain Res. *840*, 23–35.

Lee, M.K., Borchelt, D.R., Kim, G., Thinakaran, G., Slunt, H.H., Ratovitski, T., Martin, L.J., Kittur, A., Gandy, S., Levey, A.I., et al. (1997). Hyperaccumulation of FAD-linked presenilin 1 variants *in vivo*. Nat. Med. *3*, 756–760.

Li, S., Hong, S., Shepardson, N.E., Walsh, D.M., Shankar, G.M., and Selkoe, D. (2009). Soluble oligomers of amyloid Beta protein facilitate hippocampal long-term depression by disrupting neuronal glutamate uptake. Neuron *62*, 788–801.

Luscher, C. and Huber, K.M. (2010). Group 1 mGluR-dependent synaptic long-term depression: mechanisms and implications for circuitry and disease. Neuron *65*, 445–459.

Malenka, R.C. and Bear, M.F. (2004). LTP and LTD: an embarrassment of riches. Neuron *44*, 5–21.

Mann, E.O. and Paulsen, O. (2007). Role of GABAergic inhibition in hippocampal network oscillations. Trends Neurosci. *30*, 343–349.

Matsuyama, S., Teraoka, R., Mori, H., and Tomiyama, T. (2007). Inverse correlation between amyloid precursor protein and synaptic plasticity in transgenic mice. Neuroreport *18*, 1083–1087.

McNaughton, B.L. (1980). Evidence for two physiologically distinct perforant pathways to the fascia dentata. Brain Res. *199*, 1–19.

Middei, S., Roberto, A., Berretta, N., Panico, M.B., Lista, S., Bernardi, G., Mercuri, N.B., Ammassari-Teule, M., and Nistico, R. (2010). Learning discloses abnormal structural and functional plasticity at hippocampal synapses in the APP23 mouse model of Alzheimer's disease. Learn. Mem. *17*, 236–240.

Mitchell, J.C., Ariff, B.B., Yates, D.M., Lau, K.F., Perkinton, M.S., Rogelj, B., Stephenson, J.D., Miller, C.C., and McLoughlin, D.M. (2009). X11β rescues memory and long-term potentiation deficits in Alzheimer's disease APPswe Tg2576 mice. Hum. Mol. Genet. *18*, 4492–4500.

Mody, I. and Pearce, R.A. (2004). Diversity of inhibitory neurotransmission through $GABA_A$ receptors. Trends Neurosci. *27*, 569–575.

Moechars, D., Dewachter, I., Lorent, K., Reverse, D., Baekelandt, V., Naidu, A., Tesseur, I., Spittaels, K., Haute, C.V., Checler, F., et al. (1999). Early phenotypic changes in transgenic mice that overexpress different mutants of amyloid precursor protein in brain. J. Biol. Chem. *274*, 6483–6492.

Morrissette, D.A., Parachikova, A., Green, K.N., and LaFerla, F.M. (2009). Relevance of transgenic mouse models to human Alzheimer disease. J. Biol. Chem. *284*, 6033–6037.

Mucke, L., Masliah, E., Yu, G.Q., Mallory, M., Rockenstein, E.M., Tatsuno, G., Hu, K., Kholodenko, D., Johnson-Wood, K., and McConlogue, L. (2000). High-level neuronal expression of Aβ 1-42 in wild-type human amyloid protein precursor transgenic mice: synaptotoxicity without plaque formation. J. Neurosci. *20*, 4050–4058.

Munton, R.P., Vizi, S., and Mansuy, I.M. (2004). The role of protein phosphatase-1 in the modulation of synaptic and structural plasticity. FEBS Lett. *567*, 121–128.

Nguyen, P.V., Abel, T., Kandel, E.R., and Bourtchouladze, R. (2000). Strain-dependent differences in LTP and hippocampus-dependent memory in inbred mice. Learn. Mem. *7*, 170–179.

Oddo, S., Caccamo, A., Shepherd, J.D., Murphy, M.P., Golde, T.E., Kayed, R., Metherate, R., Mattson, M.P., Akbari, Y., and LaFerla, F.M. (2003). Triple-transgenic model of Alzheimer's disease with plaques and tangles: intracellular Aβ and synaptic dysfunction. Neuron *39*, 409–421.

Palop, J.J. and Mucke, L. (2010). Amyloid-β-induced neuronal dysfunction in Alzheimer's disease: from synapses toward neural networks. Nat. Neurosci. *13*, 812–818.

Palop, J.J., Chin, J., Roberson, E.D., Wang, J., Thwin, M.T., Bien-Ly, N., Yoo, J., Ho, K.O., Yu, G.Q., Kreitzer, A., et al. (2007). Aberrant excitatory neuronal activity and compensatory remodeling of inhibitory hippocampal circuits in mouse models of Alzheimer's disease. Neuron *55*, 697–711.

Parent, A., Linden, D.J., Sisodia, S.S., and Borchelt, D.R. (1999). Synaptic transmission and hippocampal long-term potentiation in transgenic mice expressing FAD-linked presenilin 1. Neurobiol. Dis. *6*, 56–62.

Perez, S.E., He, B., Muhammad, N., Oh, K.J., Fahnestock, M., Ikonomovic, M.D., and Mufson, E.J. (2011). Cholinotrophic basal forebrain system alterations in 3xTg-AD transgenic mice. Neurobiol. Dis. *41*, 338–352.

Pinard, A., Seddik, R., and Bettler, B. (2010). GABAB receptors: physiological functions and mechanisms of diversity. Adv. Pharmacol. *58*, 231–255.

Postina, R., Schroeder, A., Dewachter, I., Bohl, J., Schmitt, U., Kojro, E., Prinzen, C., Endres, K., Hiemke, C., Blessing, M., et al. (2004). A disintegrin-metalloproteinase prevents amyloid plaque formation and hippocampal defects in an Alzheimer disease mouse model. J. Clin. Invest. *113*, 1456–1464.

Radde, R., Bolmont, T., Kaeser, S.A., Coomaraswamy, J., Lindau, D., Stoltze, L., Calhoun, M.E., Jaggi, F., Wolburg, H., Gengler, S., et al. (2006). Aβ42-driven cerebral amyloidosis in transgenic mice reveals early and robust pathology. EMBO Rep. *7*, 940–946.

Richardson, J.C., Kendal, C.E., Anderson, R., Priest, F., Gower, E., Soden, P., Gray, R., Topps, S., Howlett, D.R., Lavender, D., et al. (2003). Ultrastructural and behavioural changes precede amyloid deposition in a transgenic model of Alzheimer's disease. Neuroscience *122*, 213–228.

Roberson, E.D., Halabisky, B., Yoo, J.W., Yao, J., Chin, J., Yan, F., Wu, T., Hamto, P., Devidze, N., Yu, G.Q., et al. (2011). Amyloid-β/Fyn-induced synaptic, network, and cognitive impairments depend on tau levels in multiple mouse models of Alzheimer's disease. J. Neurosci. *31*, 700–711.

Roder, S., Danober, L., Pozza, M.F., Lingenhoehl, K., Wiederhold, K.H., and Olpe, H.R. (2003). Electrophysiological studies on the hippocampus and prefrontal cortex assessing the effects of amyloidosis in amyloid precursor protein 23 transgenic mice. Neuroscience *120*, 705–720.

Rosato-Siri, M., Cattaneo, A., and Cherubini, E. (2006). Nicotine-induced enhancement of synaptic plasticity at CA3-CA1 synapses requires GABAergic interneurons in adult anti-NGF mice. J. Physiol. *576*, 361–377.

Ruberti, F., Capsoni, S., Comparini, A., Di Daniel, E., Franzot, J., Gonfloni, S., Rossi, G., Berardi, N., and Cattaneo, A. (2000). Phenotypic knockout of nerve growth factor in adult transgenic mice reveals severe deficits in basal forebrain cholinergic neurons, cell death in the spleen, and skeletal muscle dystrophy. J. Neurosci. *20*, 2589–2601.

Saganich, M.J., Schroeder, B.E., Galvan, V., Bredesen, D.E., Koo, E.H., and Heinemann, S.F. (2006). Deficits in synaptic transmission and learning in amyloid precursor protein (APP) transgenic mice require C-terminal cleavage of APP. J. Neurosci. *26*, 13428–13436.

Schneider, I., Reverse, D., Dewachter, I., Ris, L., Caluwaerts, N., Kuiperi, C., Gilis, M., Geerts, H., Kretzschmar, H., Godaux, E., et al. (2001). Mutant presenilins disturb neuronal calcium homeostasis in the brain of transgenic mice, decreasing the threshold for excitotoxicity and facilitating long-term potentiation. J. Biol. Chem. *276*, 11539–11544.

Seabrook, G.R., Easter, A., Dawson, G.R., and Bowery, B.J. (1997). Modulation of long-term potentiation in CA1 region of mouse hippocampal brain slices by $GABA_A$ receptor benzodiazepine site ligands. Neuropharmacology *36*, 823–830.

Selkoe, D.J. (2002). Alzheimer's disease is a synaptic failure. Science *298*, 789–791.

Shankar, G.M., Li, S., Mehta, T.H., Garcia-Munoz, A., Shepardson, N.E., Smith, I., Brett, F.M., Farrell, M.A., Rowan, M.J., Lemere, C.A., et al. (2008). Amyloid-β protein dimers isolated directly from Alzheimer's brains impair synaptic plasticity and memory. Nat. Med. *14*, 837–842.

Sivilotti, L. and Nistri, A. (1991). GABA receptor mechanisms in the central nervous system. Prog. Neurobiol. *36*, 35–92.

Sola, E., Capsoni, S., Rosato-Siri, M., Cattaneo, A., and Cherubini, E. (2006). Failure of nicotine-dependent enhancement of synaptic efficacy at Schaffer-collateral CA1 synapses of AD11 anti-nerve growth factor transgenic mice. Eur. J. Neurosci. *24*, 1252–1264.

Sturchler-Pierrat, C., Abramowski, D., Duke, M., Wiederhold, K.H., Mistl, C., Rothacher, S., Ledermann, B., Burki, K., Frey, P., Paganetti, P.A., et al. (1997). Two amyloid precursor protein transgenic mouse models with Alzheimer disease-like pathology. Proc. Natl. Acad. Sci. USA *94*, 13287–13292.

Sun, B., Zhou, Y., Halabisky, B., Lo, I., Cho, S.H., Mueller-Steiner, S., Devidze, N., Wang, X., Grubb, A., and Gan, L. (2008). Cystatin C-cathepsin B axis regulates amyloid β levels and associated neuronal deficits in an animal model of Alzheimer's disease. Neuron *60*, 247–257.

Tampellini, D., Rahman, N., Gallo, E.F., Huang, Z., Dumont, M., Capetillo-Zarate, E., Ma, T., Zheng, R., Lu, B., Nanus, D.M., et al. (2009). Synaptic activity reduces intraneuronal Abeta, promotes APP transport to synapses, and protects against Aβ-related synaptic alterations. J. Neurosci. *29*, 9704–9713.

Townsend, M., Shankar, G.M., Mehta, T., Walsh, D.M., and Selkoe, D.J. (2006). Effects of secreted oligomers of amyloid β-protein on hippocampal synaptic plasticity: a potent role for trimers. J. Physiol. *572*, 477–492.

Trinchese, F., Liu, S., Battaglia, F., Walter, S., Mathews, P.M., and Arancio, O. (2004). Progressive age-related development of Alzheimer-like pathology in APP/PS1 mice. Ann. Neurol. *55*, 801–814.

Trinchese, F., Fa', M., Liu, S., Zhang, H., Hidalgo, A., Schmidt, S.D., Yamaguchi, H., Yoshii, N., Mathews, P.M., Nixon, R.A., et al. (2008). Inhibition of calpains improves memory and synaptic transmission in a mouse model of Alzheimer disease. J. Clin. Invest. *118*, 2796–2807.

Volianskis, A., Kostner, R., Molgaard, M., Hass, S., and Jensen, M.S. (2010). Episodic memory deficits are not related to altered glutamatergic synaptic transmission and plasticity in the CA1 hippocampus of the APPswe/PS1δE9-deleted transgenic mice model of ss-amyloidosis. Neurobiol. Aging *31*, 1173–1187.

Walsh, D.M., Klyubin, I., Fadeeva, J.V., Cullen, W.K., Anwyl, R., Wolfe, M.S., Rowan, M.J., and Selkoe, D.J. (2002). Naturally secreted oligomers of amyloid beta protein potently inhibit hippocampal long-term potentiation *in vivo*. Nature *416*, 535–539.

Wang, H.Y., Lee, D.H., D'Andrea, M.R., Peterson, P.A., Shank, R.P., and Reitz, A.B. (2000a). β-Amyloid(1-42) binds to α7 nicotinic acetylcholine receptor with high affinity. Implications for Alzheimer's disease pathology. J. Biol. Chem. *275*, 5626–5632.

Wang, H.Y., Lee, D.H., Davis, C.B., and Shank, R.P. (2000b). Amyloid peptide Aβ(1-42) binds selectively and with picomolar affinity to α7 nicotinic acetylcholine receptors. J. Neurochem. *75*, 1155–1161.

Wang, Y., Greig, N.H., Yu, Q.S., and Mattson, M.P. (2009). Presenilin-1 mutation impairs cholinergic modulation of synaptic plasticity and suppresses NMDA currents in hippocampus slices. Neurobiol. Aging *30*, 1061–1068.

Wang, H.W., Pasternak, J.F., Kuo, H., Ristic, H., Lambert, M.P., Chromy, B., Viola, K.L., Klein, W.L., Stine, W.B., Krafft, G.A., et al. (2002). Soluble oligomers of β amyloid (1-42) inhibit long-term potentiation but not long-term depression in rat dentate gyrus. Brain Res. *924*, 133–140.

Wei, W., Nguyen, L.N., Kessels, H.W., Hagiwara, H., Sisodia, S., and Malinow, R. (2010). Amyloid β from axons and dendrites reduces local spine number and plasticity. Nat. Neurosci. *13*, 190–196.

Whitlock, J.R., Heynen, A.J., Shuler, M.G., and Bear, M.F. (2006). Learning induces long-term potentiation in the hippocampus. Science *313*, 1093–1097.

Wigstrom, H. and Gustafsson, B. (1986). Postsynaptic control of hippocampal long-term potentiation. J. Physiol. (Paris) *81*, 228–236.

Wisniewski, T. and Sigurdsson, E.M. (2010). Murine models of Alzheimer's disease and their use in developing immunotherapies. Biochim. Biophys. Acta *1802*, 847–859.

Wyss-Coray, T., Masliah, E., Mallory, M., McConlogue, L., Johnson-Wood, K., Lin, C., and Mucke, L. (1997). Amyloidogenic role of cytokine TGF-beta1 in transgenic mice and in Alzheimer's disease. Nature *389*, 603–606.

Yoshiike, Y., Kimura, T., Yamashita, S., Furudate, H., Mizoroki, T., Murayama, M., and Takashima, A. (2008). $GABA_A$ receptor-mediated acceleration of aging-associated memory decline in APP/PS1 mice and its pharmacological treatment by picrotoxin. PLoS One *3*, e3029.

Zaman, S.H., Parent, A., Laskey, A., Lee, M.K., Borchelt, D.R., Sisodia, S.S., and Malinow, R. (2000). Enhanced synaptic potentiation in transgenic mice expressing presenilin 1 familial Alzheimer's disease mutation is normalized with a benzodiazepine. Neurobiol. Dis. *7*, 54–63.

Zucker, R.S. and Regehr, W.G. (2002). Short-term synaptic plasticity. Annu. Rev. Physiol. *64*, 355–405.

Received March 25, 2011; accepted April 15, 2011; previously published online July 6, 2011